Cirrus clouds, ice supersaturation, and their dynamical background

Klaus Gierens and Sina Hofer
DLR Oberpfaffenhofen
Institut für Physik der Atmosphäre

This work has received funding from the European Union's Horizon 2020 research and innovation programme under grant agreement No 875036

Types of ice clouds and their relation to ice supersaturation

Liquid origin cirrus:

predecessor water cloud is at water saturation → in-cloud ice supersaturation

In-situ cirrus:

rising airmass cools, relative humidity increases to ISS sufficient for ice nucleation

Contrails:

can be produced even in totally dry air. Persistence (i.e. longevity) needs ice supersaturation or nearly ice supersaturation.

Forecast of ice supersaturation – currently a great challenge

- water vapour field is quite variable with strong gradients
- water undergoes phase transitions
- water involved in atm. chemistry
- ISS is an extremal state

- NWP models treat Ci and ISS in a simplified way
- Lack of RHi measurements in the tropopause regions for data assimilation
- satellite retrievals involve strong averaging

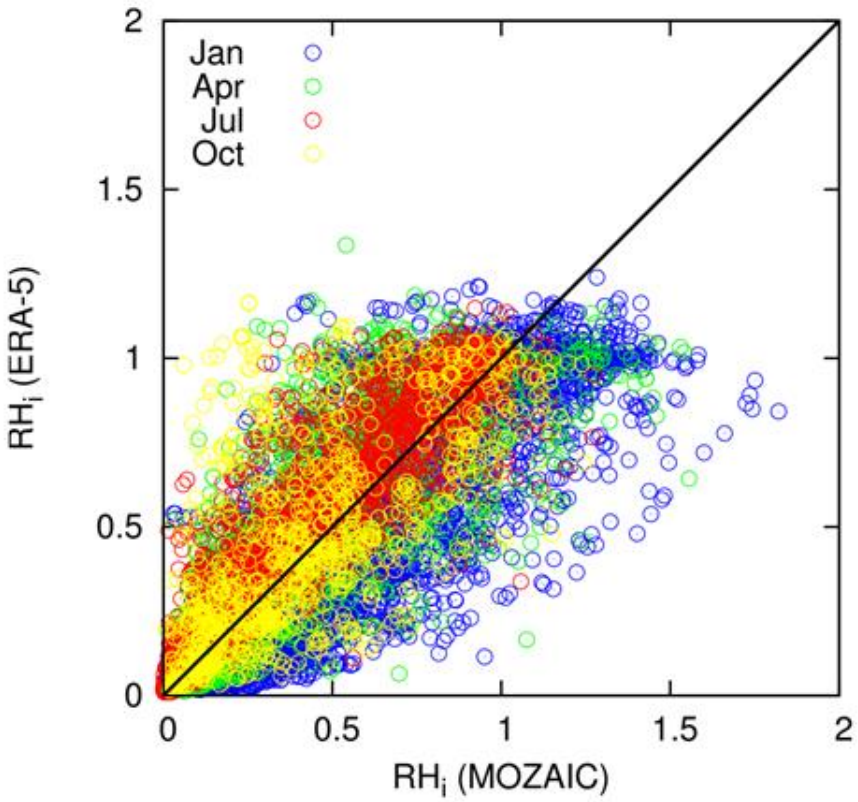

Gierens et al., 2020

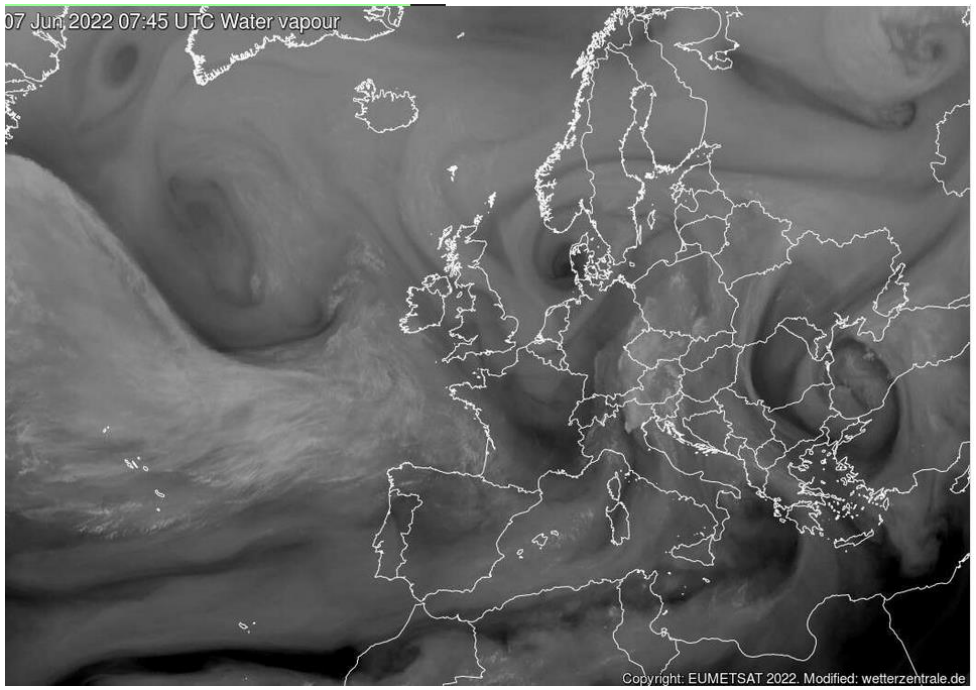

source: Eumetsat

Upper tropospheric humidity

Meteosat-7
WV Channel
20 October 1998
12:00 UTC

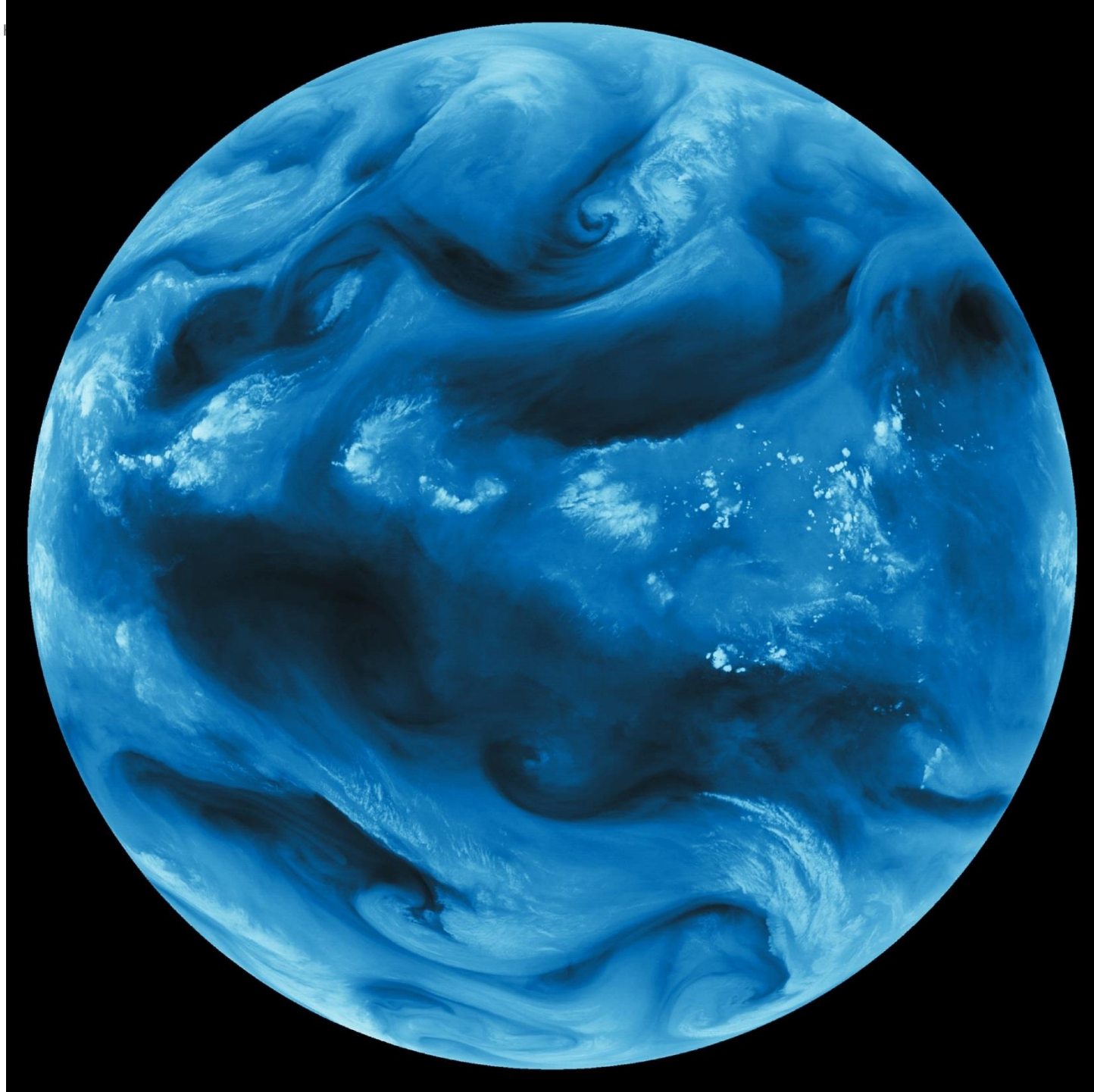

UTH and ice supersaturation (UTHi)

- >40 yrs time series of HIRS ch. 12 data on NOAA and METOP satellites
- unfortuately, the instrument was „slightly changed“ from NOAA14 to NOAA15, with severe consequences, e.g. an
- unphysical trend in the occurrence frequency of ice supersaturation

- Gierens and Eleftheratos, 2017

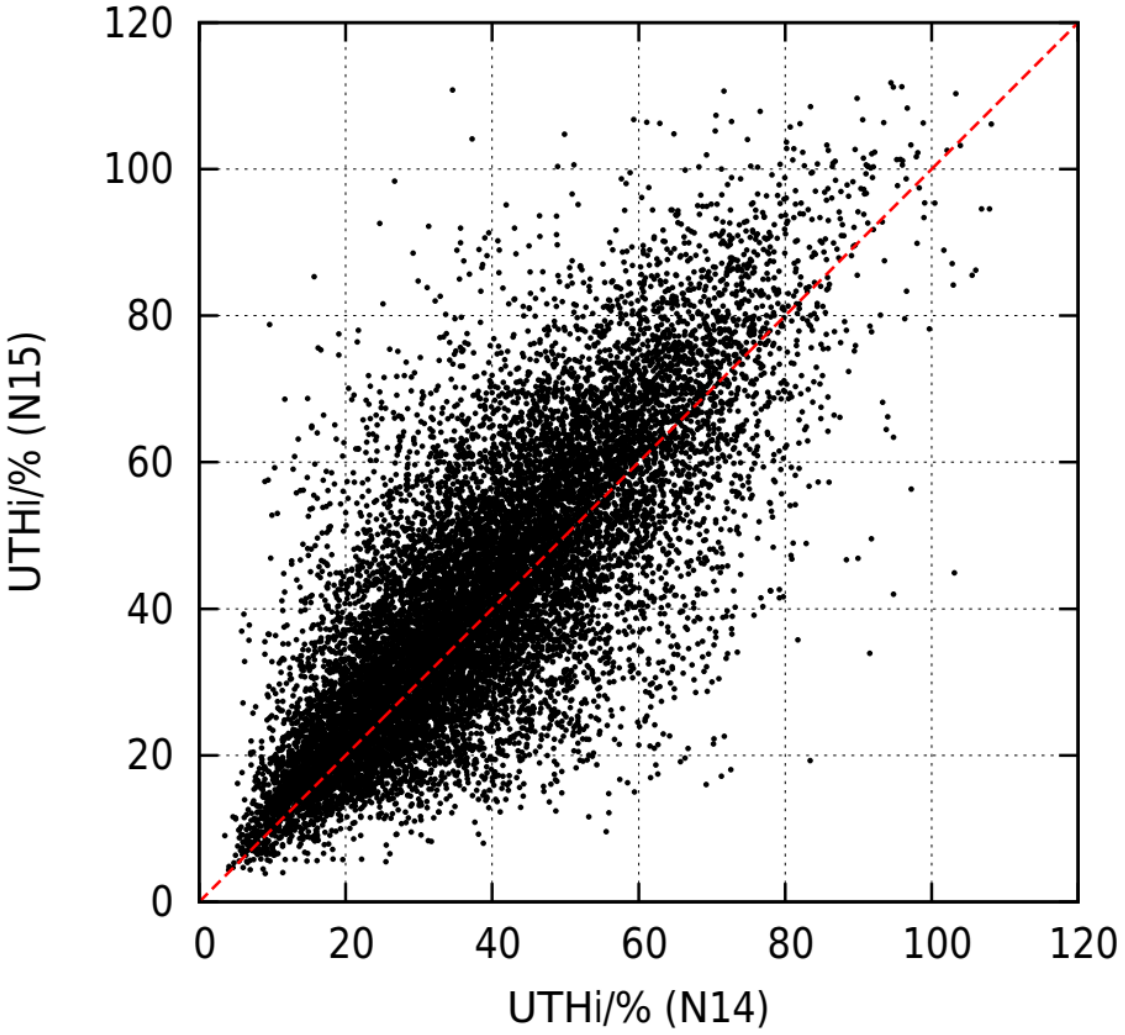

Determination and significance of UTH

- UTH determination using application of radiative transfer to the IR water vapour band (6-7µm)
- plus simplifiying assumptions on the temperature profile through the upper troposphere (linearisation)
- yields an analytical expression of the radiation intensity (brightness temperature) which can be translated into UTH or UTHi (Soden and Bretherton 1993, Stephens et al. 1996, Jackson and Bates 2001):

$$I_1 = B_0 C_\lambda \beta \int_{-\infty}^{\infty} \exp\left(-A'_\lambda \sqrt{U}\, e^{(\beta\kappa+1)\,x/2}\right) \exp(C_\lambda \beta\, x)\, \mathrm{d}x,$$

- this formula turned out to work bad in the high-U end of the distirbution (i.e. for supersaturation). Thus, the simplifiying assumtions on the temperature profile were relaxed (2nd order profile, Gierens and Eleftheratos 2020), which yields:

$$I = B_0 C_\lambda \beta \int_{-\infty}^{\infty} \exp\left\{-A_\lambda \sqrt{U}\, \left[1 + \mathrm{erf}\left(\sqrt{\kappa}\,\beta\, x - \sqrt{\kappa}/2\right)\right]^{1/2}\right\} \exp[C_\lambda(\beta\, x - \beta^2\, x^2)]\,(1 - 2\beta\, x)\, \mathrm{d}x.$$

From radiances to brightness temperatures to UTH(i)

$$T_{12} = \frac{T_0}{1 - \ln(I/B_0)/C_\lambda}$$

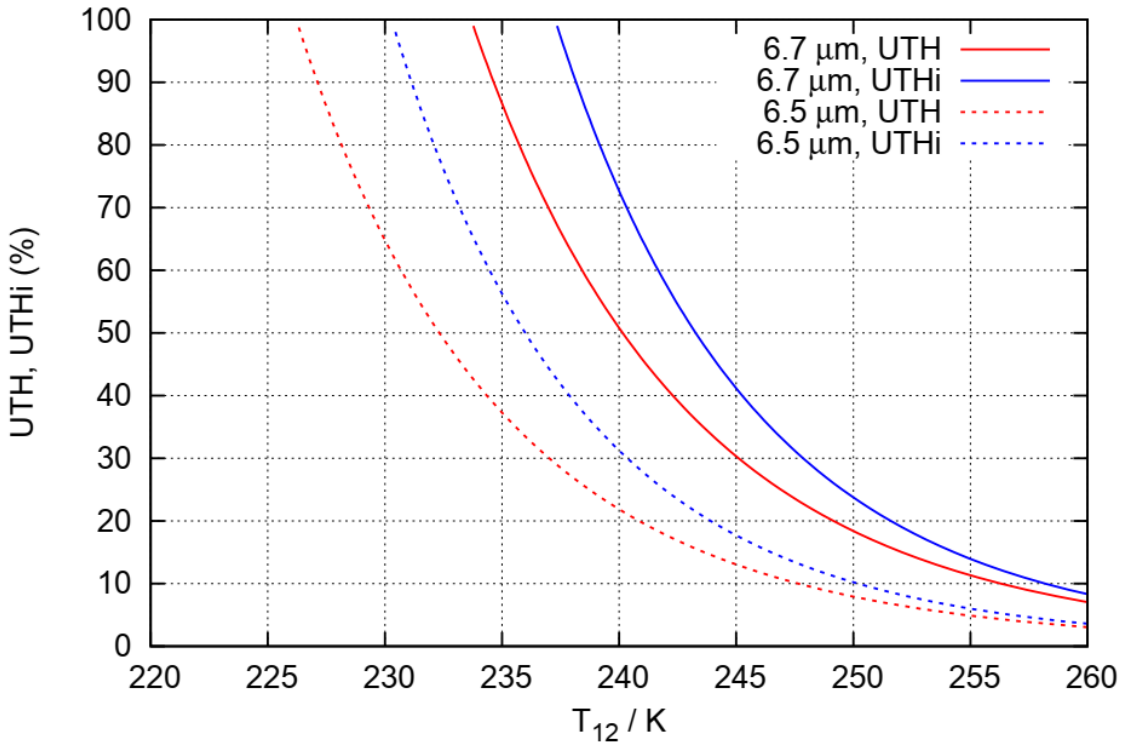

For practical purposes:

$$U/\% = 100\,\frac{\exp\left(a + bT_{12} + cT_{12}^2\right)}{a' + b'\,T_6}$$

Significance of UTH(i)

- Recall: $I = \int \Phi(x; U) \mathrm{d}\, x$
- I is the radiance measured by a water vapour channel on a satellite (e.g. HIRS).
- It is a result of the complete physics of radiative tranfer (RT) in a real atmosphere.
- U is the quantity, that must be inserted into Φ in order to fulfill the equation exactly. U is then the value of UTH.
- Φ does not represent the real atmosphere nor does it represent a complete RT. U is the UTH of a pseudo-atmosphere which reproduces the measured radiance in a simplified RT setting.
- Φ is not unique (cf. 1st-order and 2nd-order). Thus, U is not unique!

- There is no proper UTH. There is only a system of emitting and absorbing water molecules that produce a radiance (brightness temperature). UTH is just a more or less arbitrary mapping of brightness temperature into the space of positive real numbers, which should fulfill certain consistency requirements.

Radiative transfer: contribution and weighting functions

Simple form of the equation of radiative transfer
with:
light intensity I
path coordinate s
emission coefficient η
extinction (absorption plus scattering) coefficient χ

$$\frac{\mathrm{d}\,I(s)}{\mathrm{d}\,s} = \eta(s) - I(s)\chi(s),$$

Formal solution: light intensity at a certain point in space s_0

$$I(s_0) = \int_{-\infty}^{s_0} \eta(s)\,\exp\left[-\int_{s}^{s_0} \chi(s')\,\mathrm{d}s'\right]\mathrm{d}s,$$

Let‘s write this in a symbolic form

$$I(s_0) = \int_{-\infty}^{s_0} \Phi(s)\,\mathrm{d}s.$$

and then we normalise it to get a probability density function:

$$\varphi(s|s_0) := \frac{\Phi(s)}{I(s_0)} = \frac{\Phi(s)}{\int_{-\infty}^{s_0} \Phi(s')\,\mathrm{d}s'}.$$

Contribution function

$\varphi(s|s_0)$ is the contribution function.
It describes the contribution of photons emerged (emitted or scattered into the ray) at s to the intensity at s_0.

Since $\varphi(s|s_0)$ is a probability density function, it allows to compute several interesting quantities

Simple moments: $$\mu_k(s_0) = \int_{-\infty}^{s_0} s^k \, \varphi(s|s_0) \, \mathrm{d}s.$$

where μ_1 is the expectation value (mean) of the emitting positions, and $\sigma_s = (\mu_2 - \mu_1^2)^{1/2}$ the corresponding standard deviation.

More general expectation values can be obtained as well, e.g. $$\overline{T}(s_0) := \int_{-\infty}^{s_0} T(s) \, \varphi(s|s_0) \, \mathrm{d}s$$

Weighting function

Alternative form of the transfer equation using

- the source function η/χ = B[T(s)] equals the Planck function in (local) thermodynamic equilibrium
- the transmission probability between s and s_0: $\mathcal{T}(s, s_0) = \exp\left[-\int_s^{s_0} \chi(t)dt\right]$

gives $$I(s_0) = \int_{-\infty}^{s_0} B[T(s)]\,\mathcal{T}(s, s_0)\chi(s)\,\mathrm{d}s.$$

where the factor $\mathcal{T}(s, s_0)\chi(s) = \frac{d\mathcal{T}(s,s_0)}{ds} = W(s, s_0)$ is the weighting function, for which a normalised form is

another probability density function $$w(s|s_0) = \frac{\Phi(s)/B[T(s)]}{\int_{-\infty}^{s_0} \frac{\Phi(s)}{B[T(s)]}\,\mathrm{d}s}$$

Relation betw. Contribution and Weighting functions

Let us compute the mean wrt. the weighting function of the Planck function along the ray s:

$$\int_{-\infty}^{s_0} B[T(s)]\, w(s|s_0)\, \mathrm{d}s = \frac{\int_{-\infty}^{s_0} \Phi(s)\, \mathrm{d}s}{\int_{-\infty}^{s_0} \frac{\Phi(s)}{B[T(s)]}\, \mathrm{d}s} = \left[\int_{-\infty}^{s_0} \frac{1}{B[T(s)]}\, \varphi(s|s_0)\, \mathrm{d}s\right]^{-1} = \overline{\left(\frac{1}{B}\right)}^{-1}.$$

The arithmetic mean of B wrt to the weighting function equals the harmonic mean of B wrt the contribution fct.

A similar slightly more complex relation holds for other quantities that vary along the ray.

These two functions are also related to the so-called Jacobians, which describe a change in $I(s_0)$ if a relevant quantity at the position s along the ray is changed.

See Gierens and Eleftheratos, 2021, Meteorol. Z.

Characteristics of the layer of Upper-tropospheric humidity (UTH)

mean pressure and width

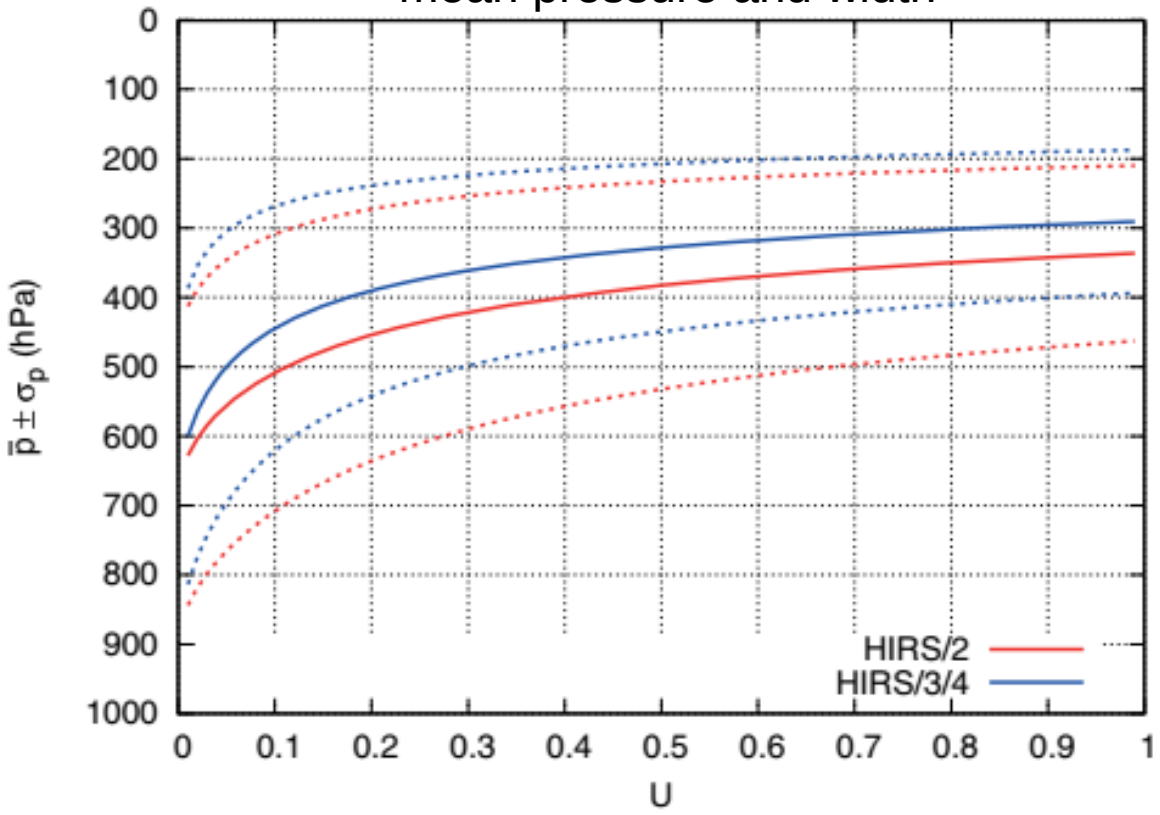

mean temperature

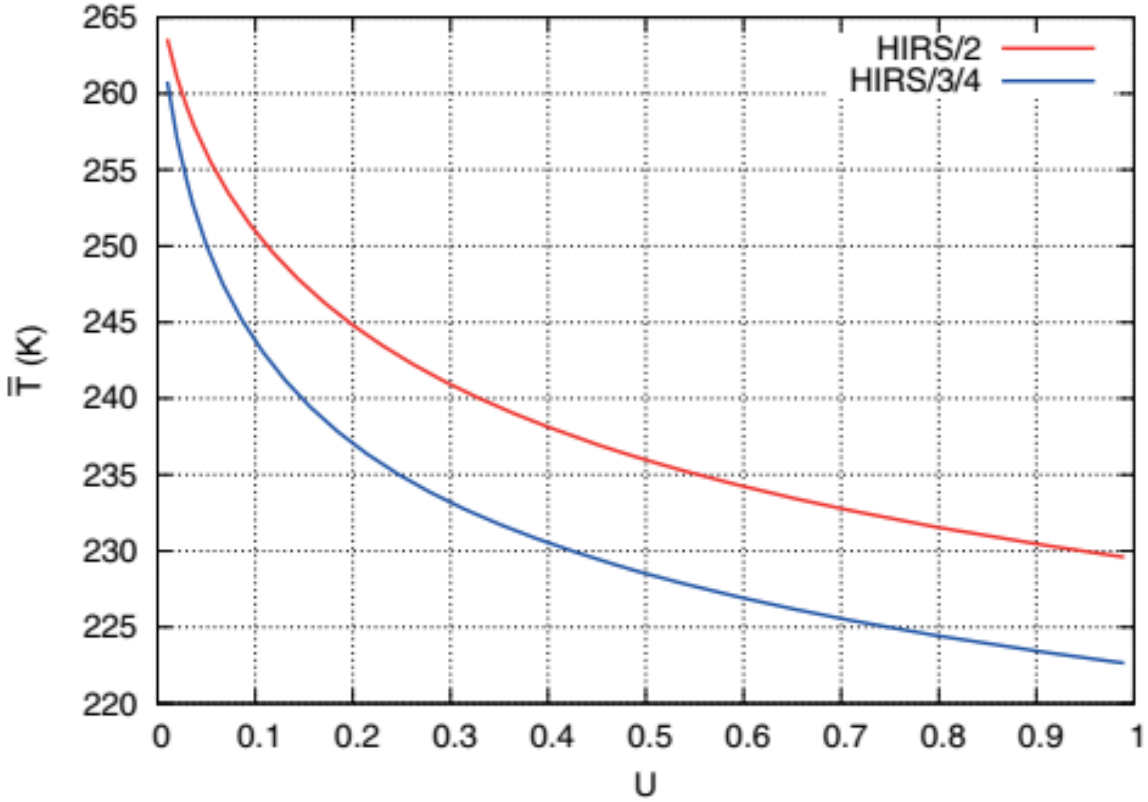

Gierens and Eleftheratos, 2021

Upper-tropospheric humidity (UTH)

Unlike RHi, UTH is a non-local quantity without sharp definition (depends on the retrieval method).

It characterises the humidity in a wide layer of the UT. The height of this layer and its thickness depend on UTH itself. Thus, given a RHi profile, one could define UTH via the contribution function and the following fixpoint equation:

$$U_\varphi = \int r(z)\,\varphi(z|U_\varphi)\,\mathrm{d}z$$

Gierens and Eleftheratos, 2021

Because of the strong averaging, satellite data show ice supersaturation rarely.

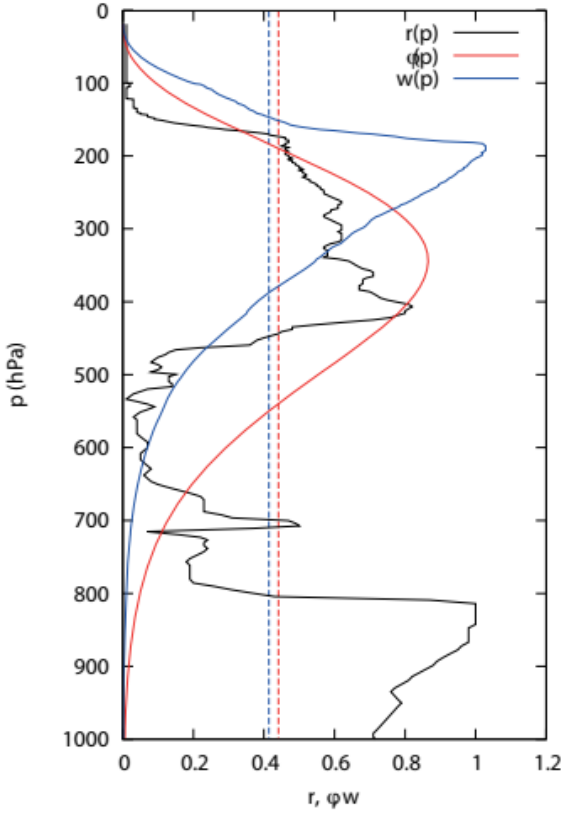

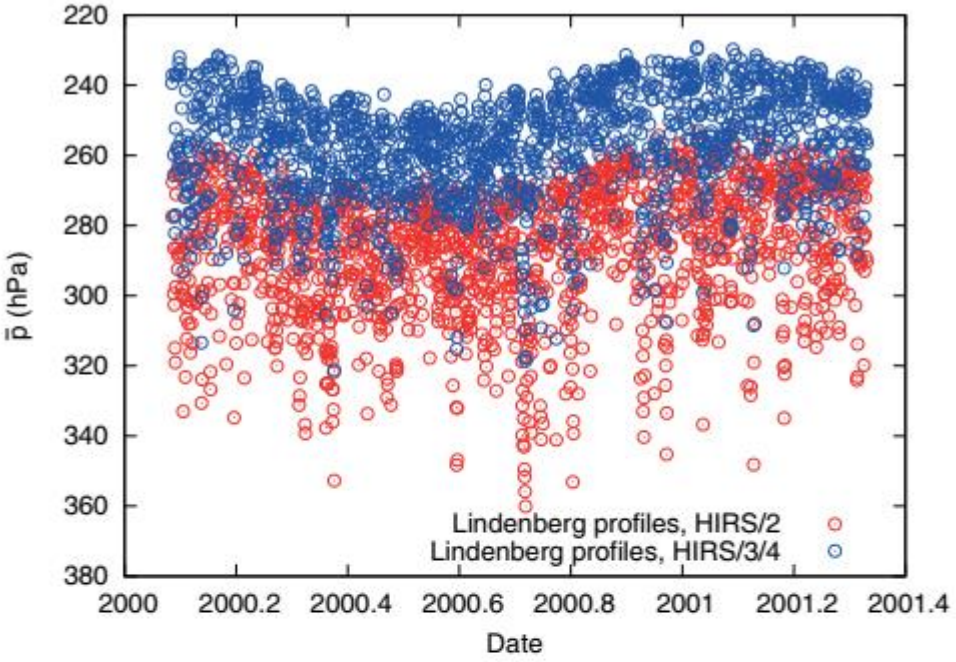

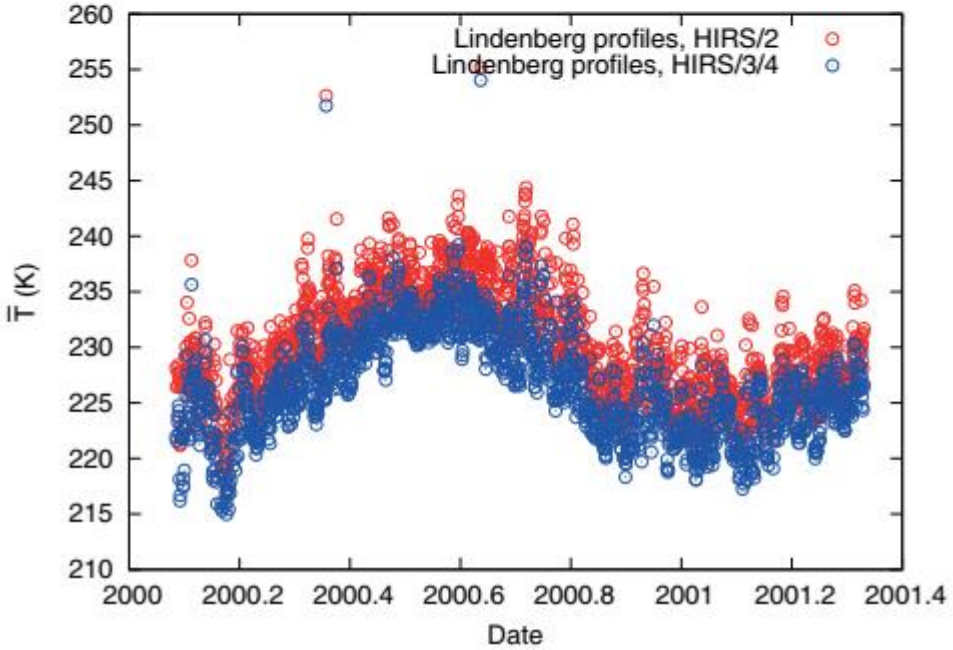

Ice supersaturated regions in dynamic regimes: case and statistical studies

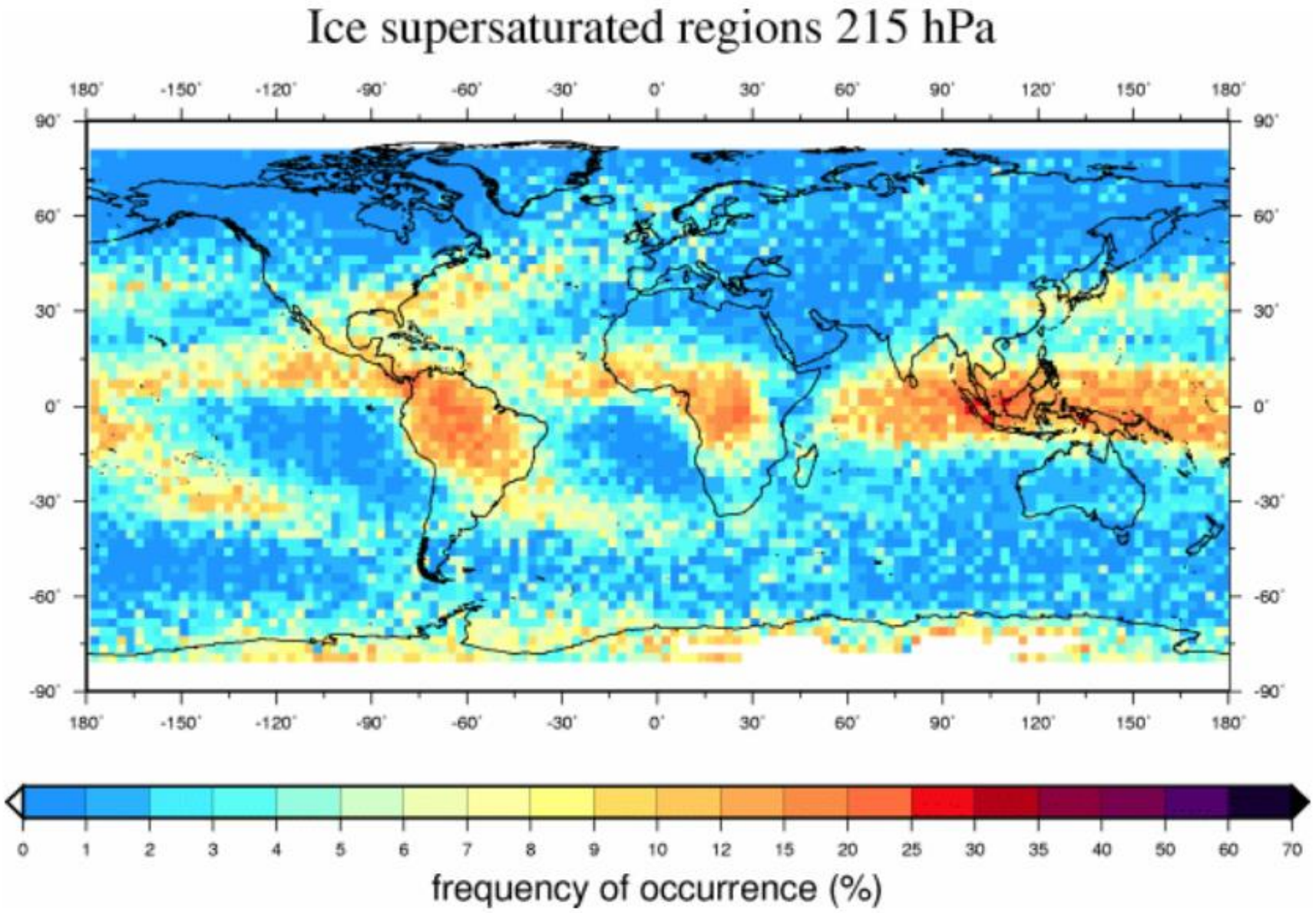

Spichtinger, Gierens & Read, 2003

In-situ and strong ascent ice supersaturation

Blue: ISSRs that were on similar altitude 2 days before, weak ascent.

Red: ISSRs that originate from strongly ascending air parcels (WCBs).

Physical differences:
WCB-derived ISS: colder and drier
weak-ascent ISS: warmer and moister

similar RHi

Spichtinger et al. 2005

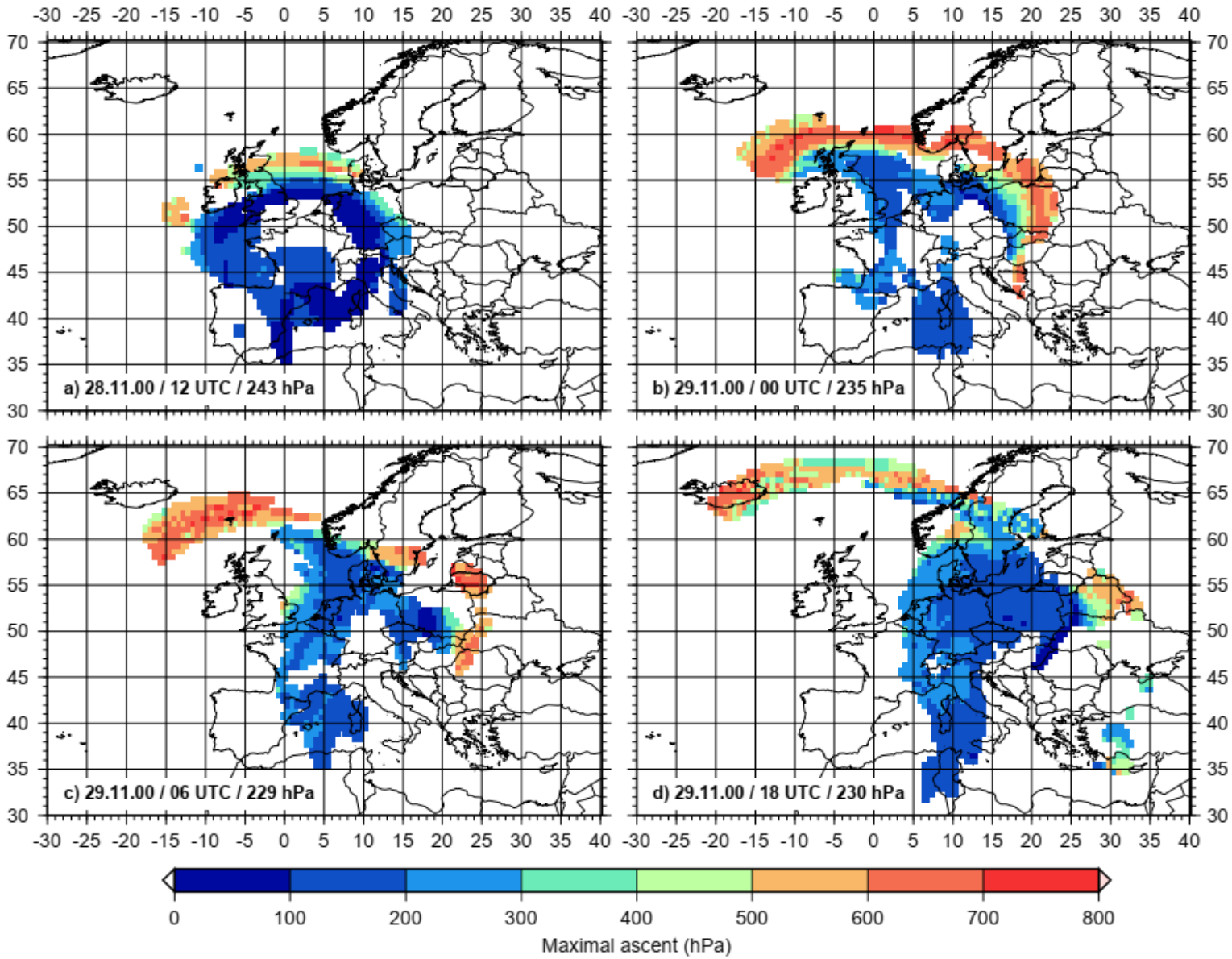

Ice supersaturation and large-scale dynamics: trajectories

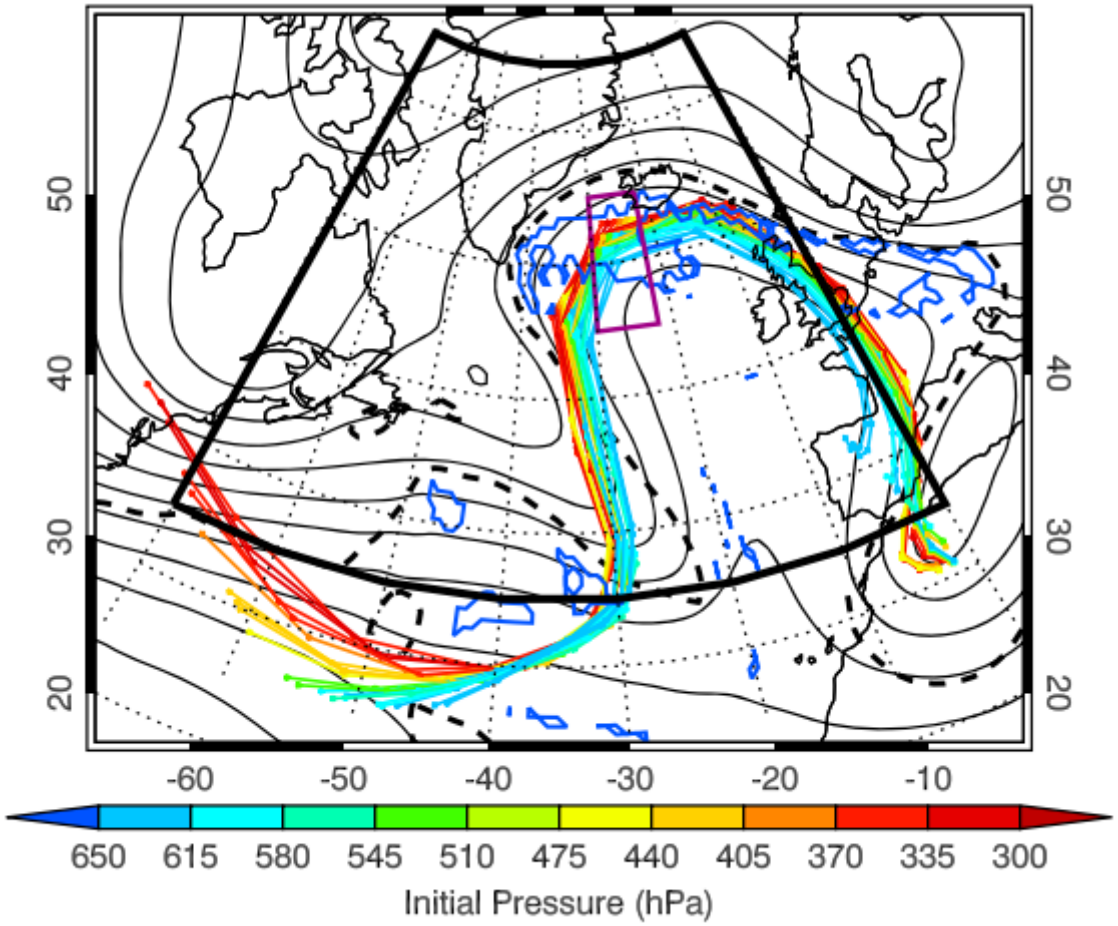

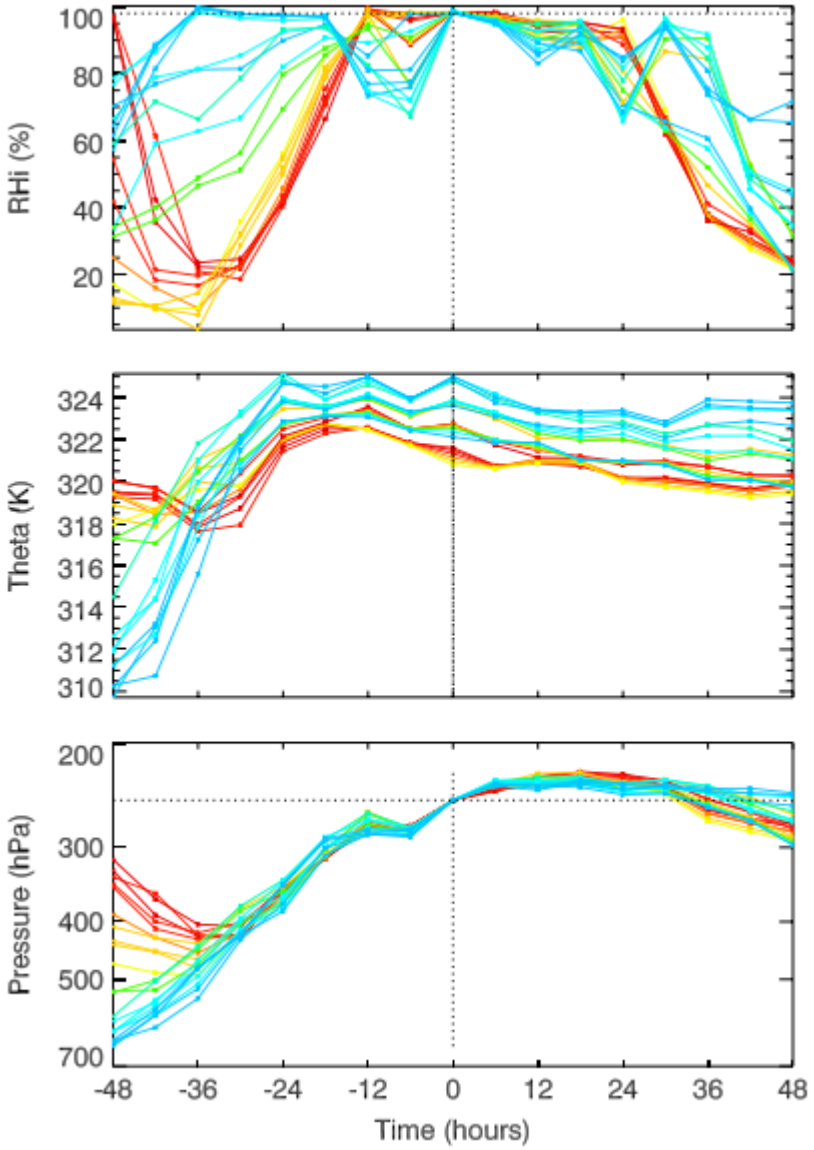

Irvine et al., JGR, 2014

Ice supersaturation and lapse rates

Atmospheric lapse rates on 21 March 2021, 18 UTC, along 52°N

$$\gamma = \frac{g}{R_d}\frac{\ln(T_0/T_1)}{\ln(p_0/p_1)}$$

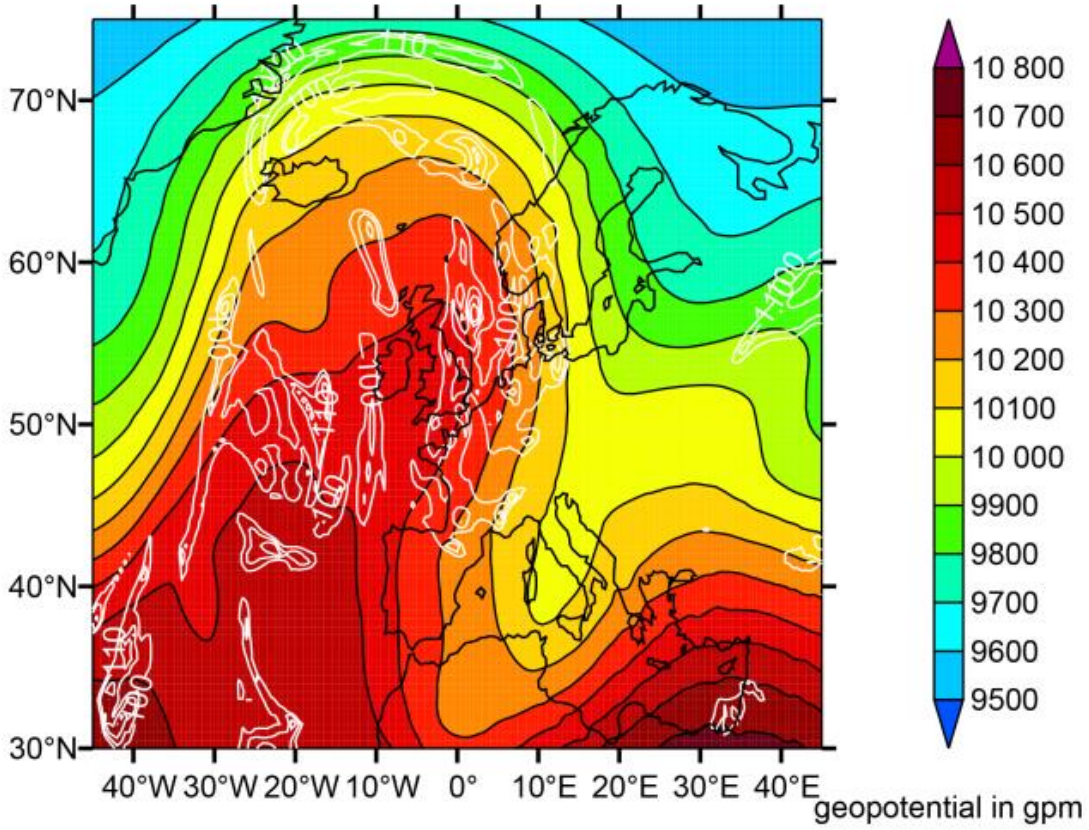

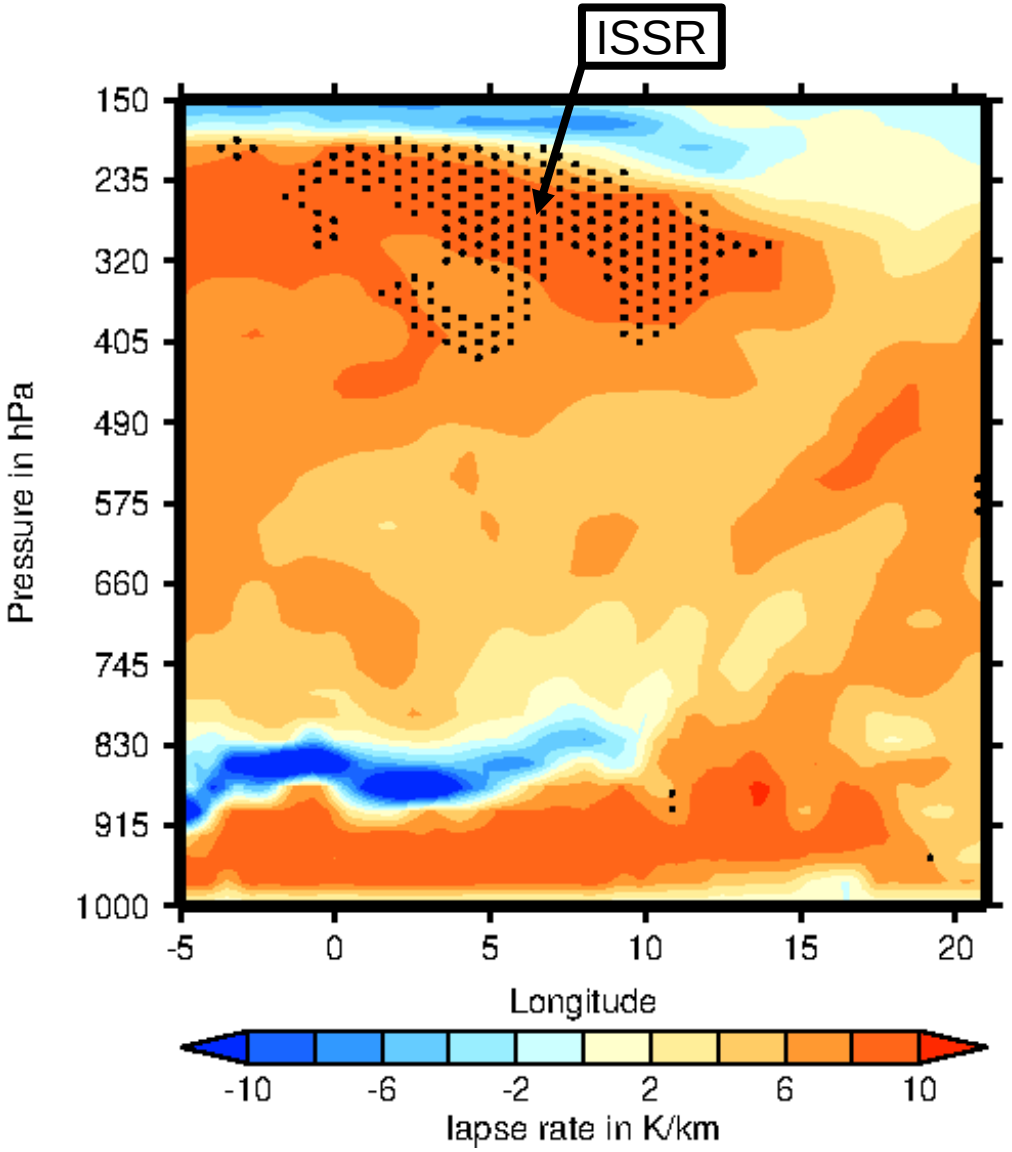

Gierens et al., 2022

Ice supersaturation, temperature and spec. humidity gradients

Life cycle of ISSRs in a $\log[e_i^*(T_{500\,\mathrm{hPa}})/e_i^*(T_{200\,\mathrm{hPa}})]$ chart
vertical temperature gradient favours ISS formation,
vertical gradient in humidity is not crucial

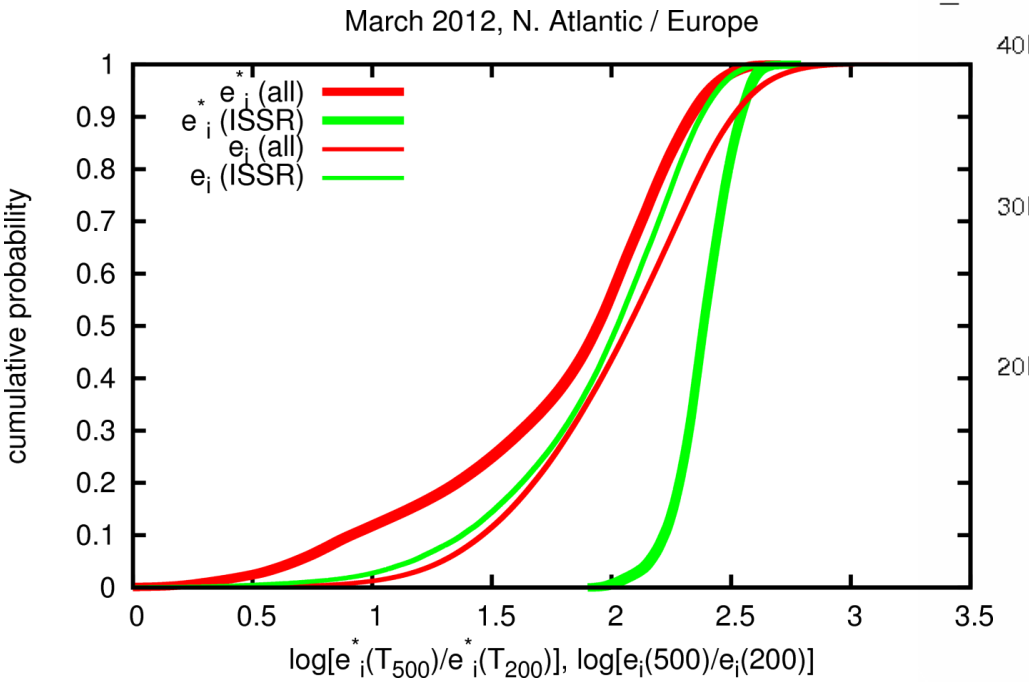

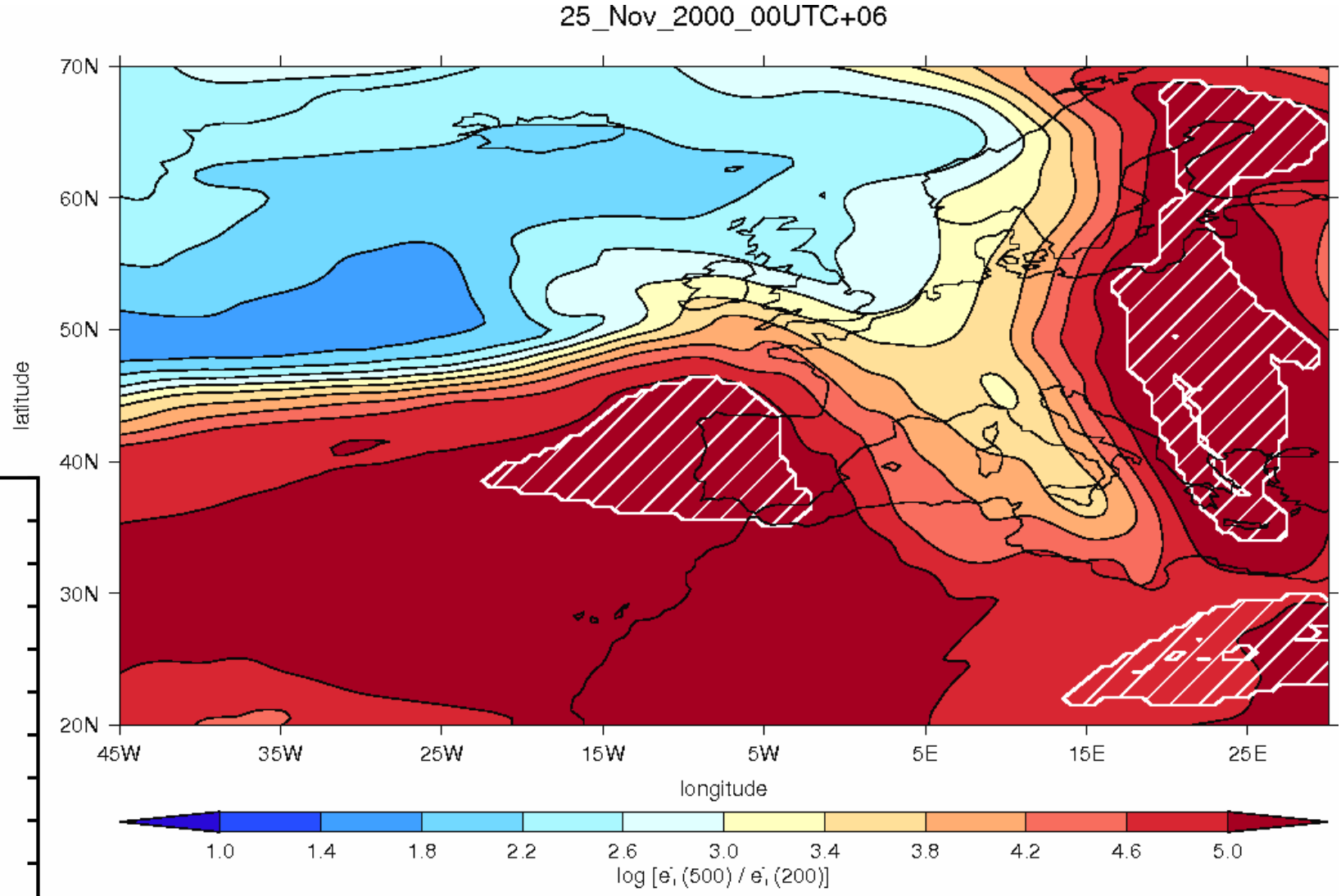

Mechanisms: Lifting (nearly adiabatic)

- Ice supersaturation and cloud formation are generally the result of lifting air masses.
- Vertical air motion changes temperature profiles and thus induces changes in the lapse rate, γ.
- T decreases faster and RHi increases faster at the upper boundary of a lifting layer (and vice versa).
- For instance, subsidence can lead to inversions, $\gamma<0$.
- Adiabatic lifting increases γ.
- As soon as condensation sets in in the upper part of a layer, the further increase of γ is slowed down.
- Instability can only be reached in layers with steeply decreasing humidity profiles (bottom moist, top dry), in other cases it is difficult to reach $\gamma>8$ K/km.
- Thus, in order to reach higher values of γ in ISSRs, another process must exist that keeps γ high and even rising.
- This is radiation.

Mechanisms: Radiation

radiation as the mechanism that leads to enhanced lapse rates in moist and supersaturated air & in thin and subvisual cirrus clouds

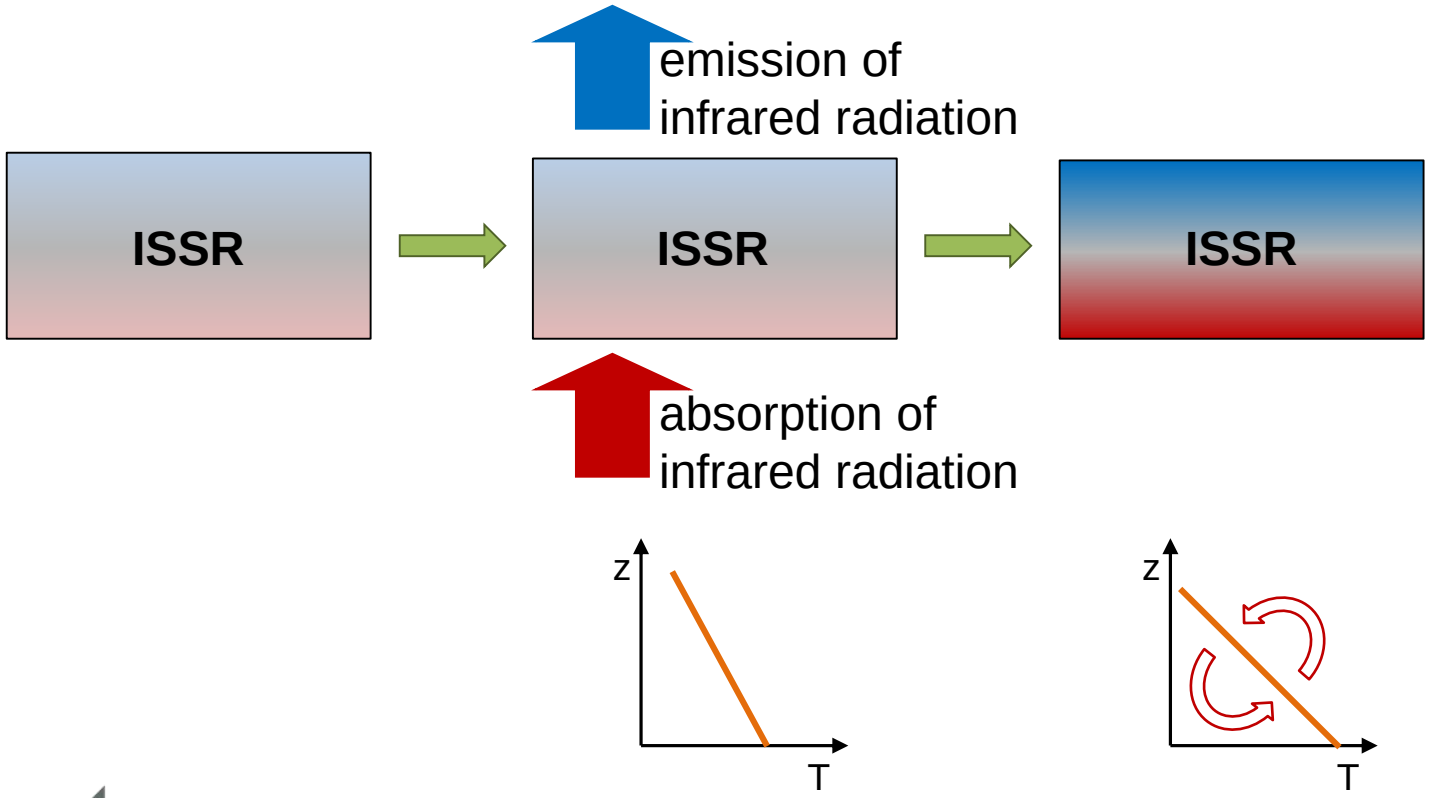

→ steepening of the temperature profile
→ increasing lapse rate

→ works for cloud free ISSRs, but gets much stronger as soon as ice is formed (ice interacts with radiation much stronger than water molecules in the gas phase)

higher-than usual lapse rates is another characteristic of ice supersaturated regions

ISS and dynamical regimes – an earlier study based on reanalysis only

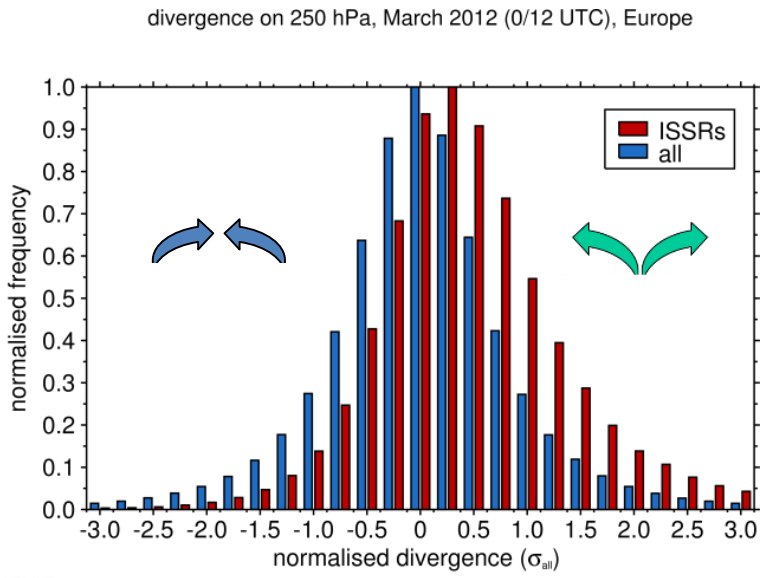

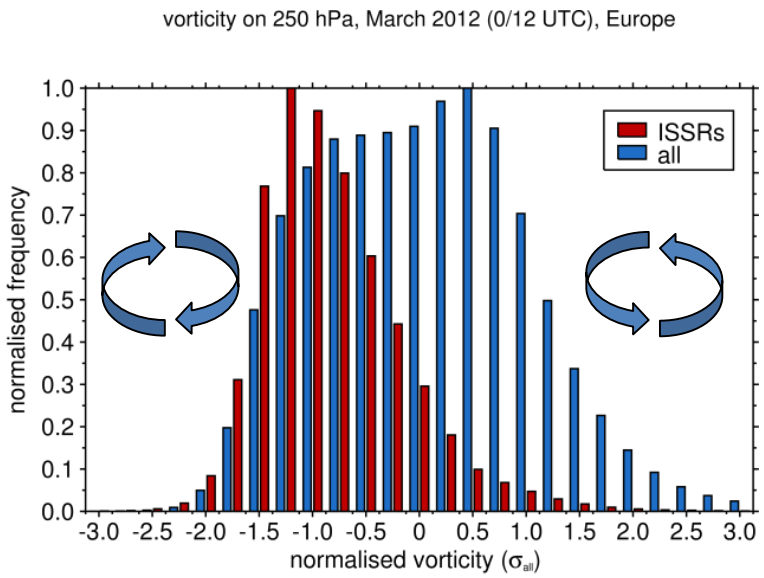

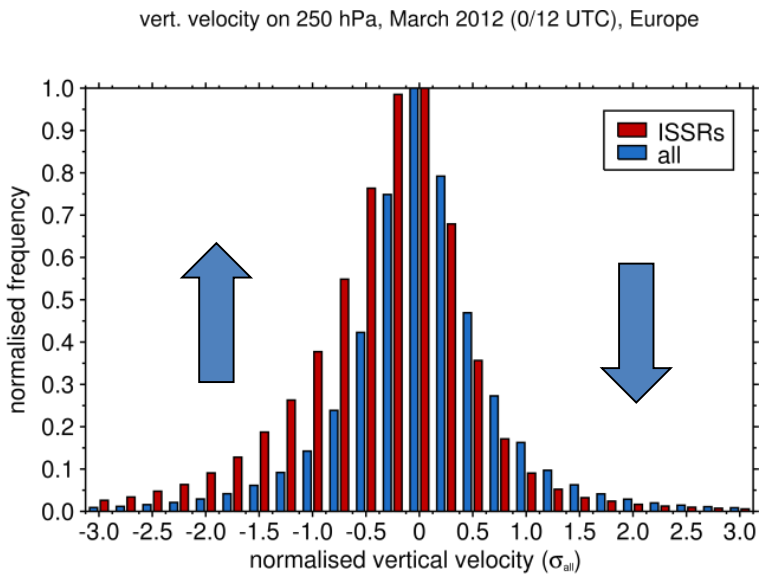

- Upward wind and divergent airflow are favourable conditions for the formation of ice supersaturation. Ice supersaturation is rare in regions with downward or convergent flow.
- ISSRs in Northern mid-latitudes are mainly confined to regions with anti-cyclonic flow.

Gierens and Brinkop, ACP, 2012

ISS and dynamical regimes – a recent study based on reanalysis and IAGOS

The dynamical fields
- Relative vorticity
- Potential vorticity
- Normalized geopotential
- Lapse rate

have distinctly differing conditional probability distributions.

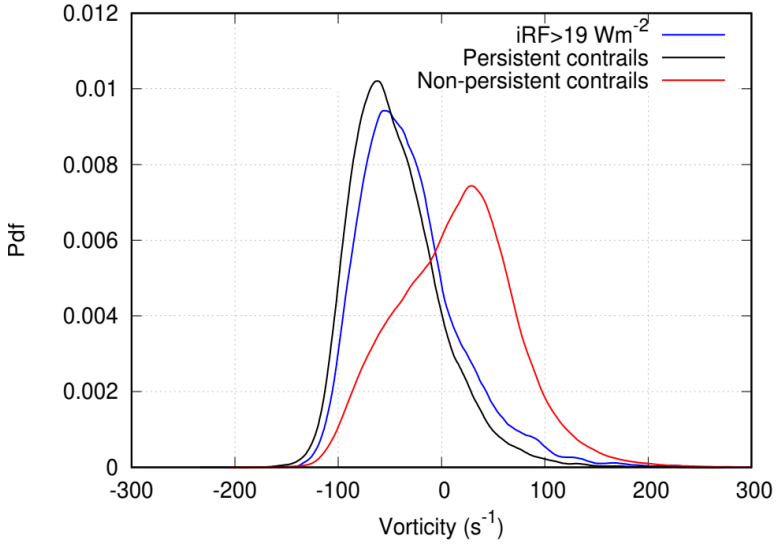

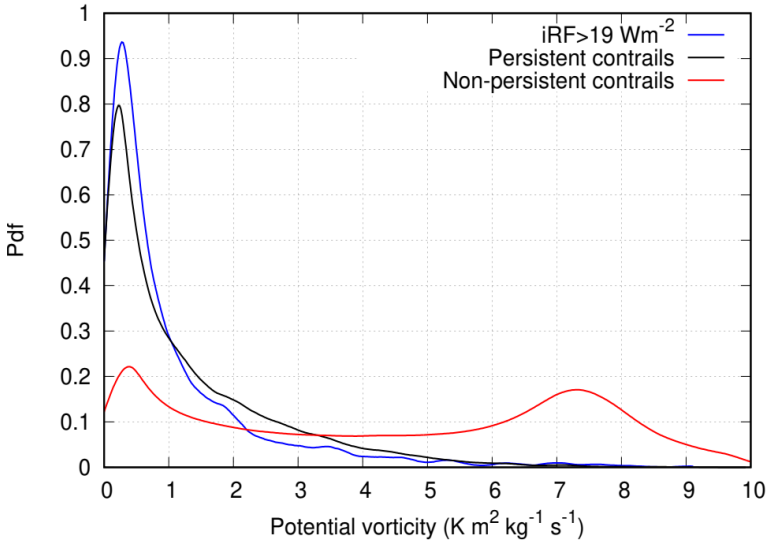

In contrast, the cond. pdfs of
- Vertical velocity
- Divergence

overlap substantially.

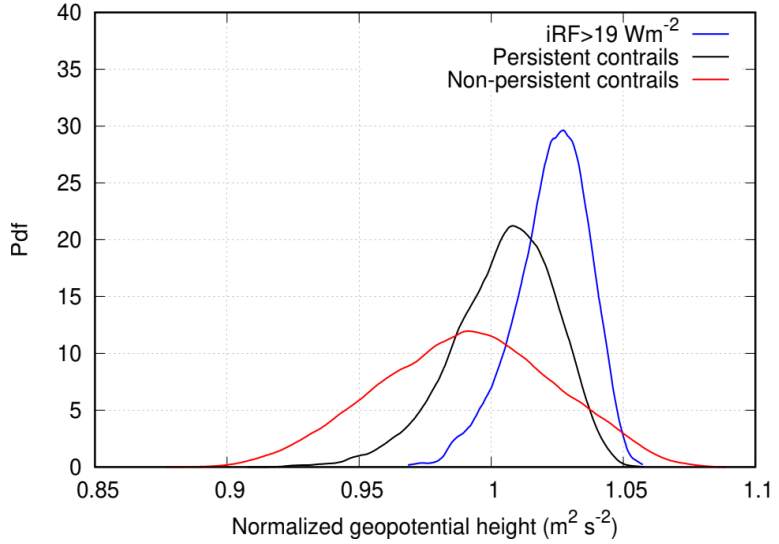

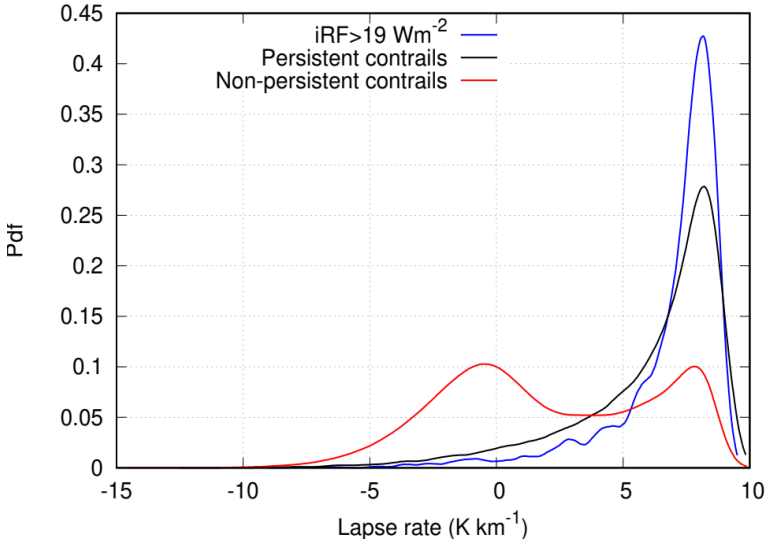

Wilhelm et al., 2022

Relations between quantities

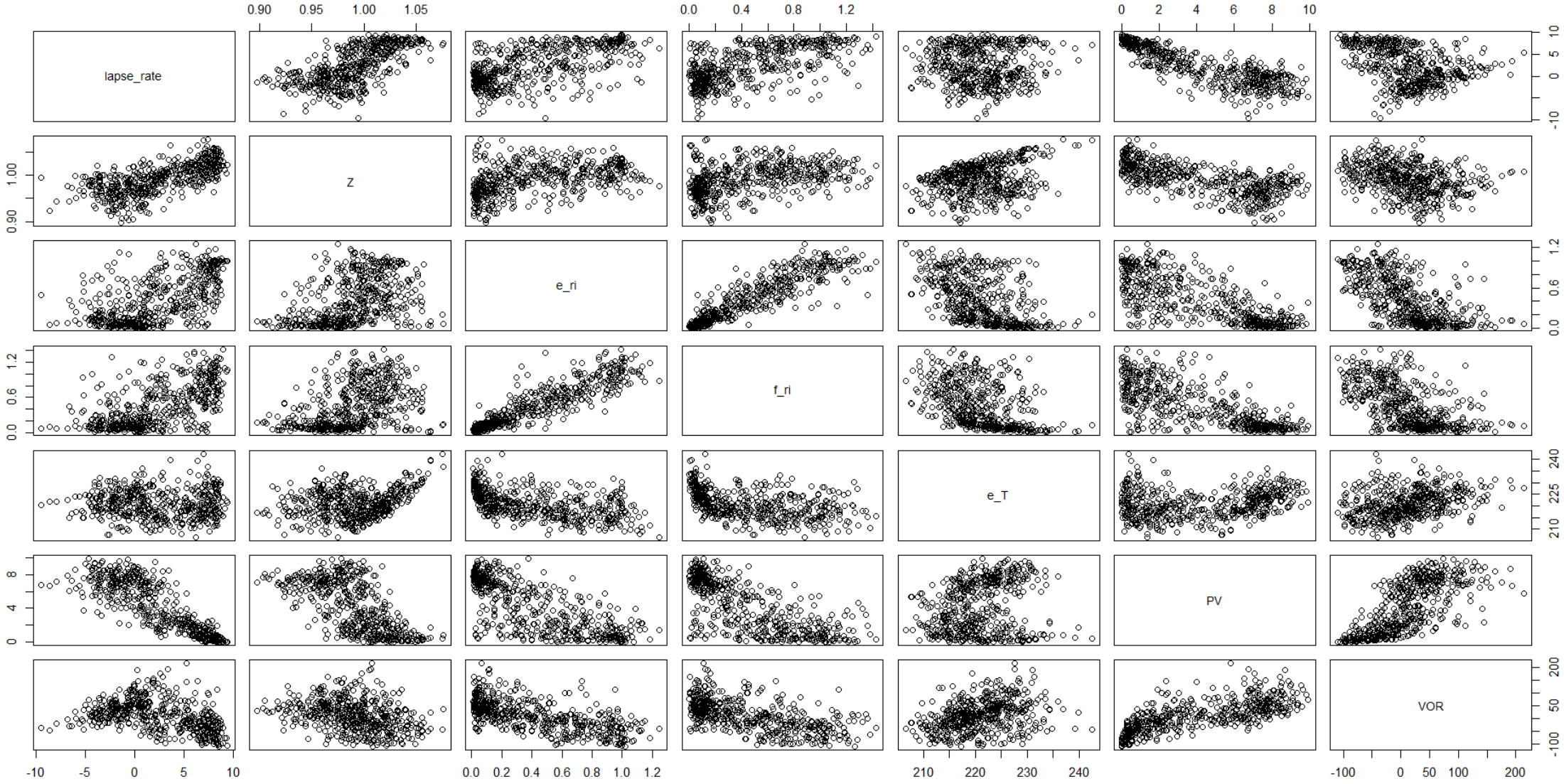

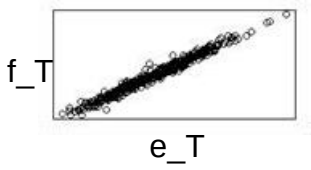

ISS prediction using dynamical proxies in a general regression

General concept of regression methods

- Statistical methods for predicting persistent contrails (“response”) depending on combinations of various dynamical proxies (“predictors”):

    1. Divide the data set (MOZAIC/IAGOS and ERA data) into a training and test data set. The presence of persistent contrails is known

    2. Train the model (= find the best coefficients for the relationships between the proxies and prediction) using the training data set

    3. Use the best coefficients/functions to predict the presence of persistent contrails in the test data set

    4. Validation of the forecast by comparing the predictions with the truth

Contingency table and scores to quantify the “success” of the method

prediction / confirmation	ISS	¬ISS
ISS	a	b
¬ISS	c	d

$$ETS = \frac{a - r}{a + b + c - r}$$

$$r = \frac{(a + b)(a + c)}{a + b + c + d}$$

ETS is symmetric in b and c, and it filters out the overwhelming influence of the default case (no/no, d).
ETS=1 → perfect prediction
ETS=0 → throw a coin for prediction
ETS=-1 → perfect prediction of the opposite

Note: success rate is not a reasonable score if the is a default case (always predict no!).

ISS prediction using dynamical proxies

GAMs (Generalized Additive Models) - Concept/Results

- general formula for a logistic regression GAM:

$$log\left(\frac{p(X)}{1-p(X)}\right) = \beta_0 + f_1(X_1) + f_2(X_2) + \ \dots + f_p(X_p)\,,$$

with: $p(X) = \Pr\ (Y = 1|X)$ and $\mathrm{X} = (X_1, X_2, \dots, X_p)$

$\Pr$: conditional probability
Y: response
X: predictors

Y is qualitative, e.g. 0 or 1
→ $p(X)$ conditional probability that the response equals 1

Application of GAMs to ISS-prediction

raw data	**0.198**
GAM predictors	ETS (threshold probability=0.34)
e_ri	0.337
e_ri, T, Z	0.375
all	0.375

The GAM-based prediction need in particular the ERA RHi. Proxy-combination without e_ri give lower ETS. However, it is not possible to raise the ETS above 0.375 with these data. Tests show that a slight improvement of the RHi fields would result in a significant rise of the ETS. Improvement here means that the conditional distributions f(e_ri|ISS) and f(e_ri|¬ISS) need greater separation. Other improvements in the form of corrections (so called Model Output Statistics, e.g. e_ri_correct=e_ri*factor or corrections using quantile matching) do not lead to improved ETS.

It seems that regression methods are not able to reliably disentangle supersaturated from subsaturated cases.

What can we learn about supersaturation from dynamical quantities (1)

We have from measurements conditioned distributions of certain quantities X, $F_{X|ISS}$ and $F_{X|\neg ISS}$ with probability density functions $f_X(x|ISS)$ and $f_X(x|\neg ISS)$.

Assume, we have a single datum $X=x_0$. Does this make ISS or non-ISS more probable?

Compare $f_X(x_0|ISS)$ and $f_X(x_0|\neg ISS)$ and select the larger of the two. Really?

No! We have to take the apriori probabilities into account, that is P(ISS) and P(¬ISS) = 1-P(ISS).

→use Bayes rule:

$$P(ISS|X=x_0) = \frac{P(x_0|ISS)\,P(ISS)}{P(x_0|ISS)P(ISS)+P(x_0|\neg ISS)P(\neg ISS)} \qquad \text{or}$$

$$P(ISS|X=x_0) = \frac{f_X(x_0|ISS)\,P(ISS)}{f_X(x_0|ISS)P(ISS)+f_X(x_0|\neg ISS)P(\neg ISS)}$$

or use the odds ratio

$$\underbrace{\frac{P(ISS|x_0)}{P(\neg ISS|x_0)}}_{\text{posterior odds ratio}} = \underbrace{\frac{f_X(x_0|ISS)}{f_X(x_0|\neg ISS)}}_{\text{likelihood ratio}}\,\underbrace{\frac{P(ISS)}{P(\neg ISS)}}_{\text{prior odds ratio}}$$

The logarithm of the odds ratio (logit) has some advantages relative to the odds ratio. Thus, we use the logit.

log-likelihood ratios for dynamical quantities: ζ, PV, Z, γ

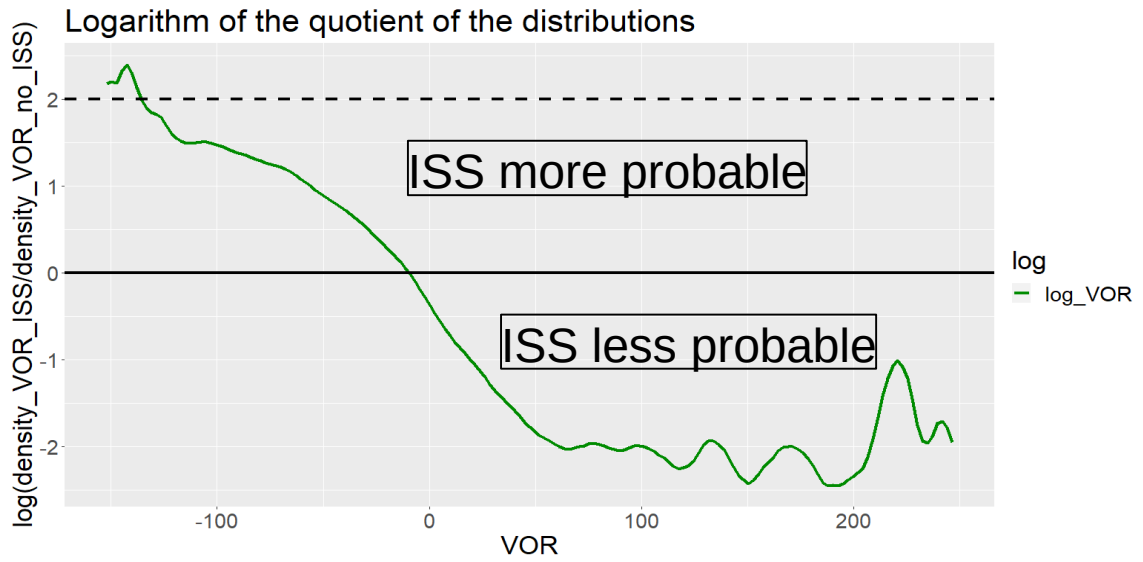

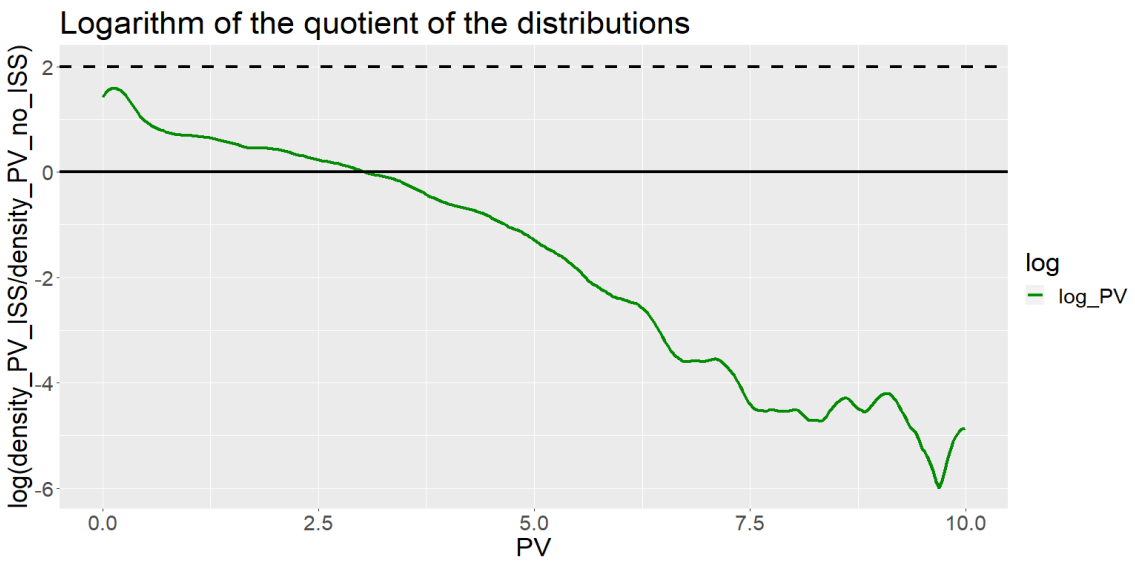

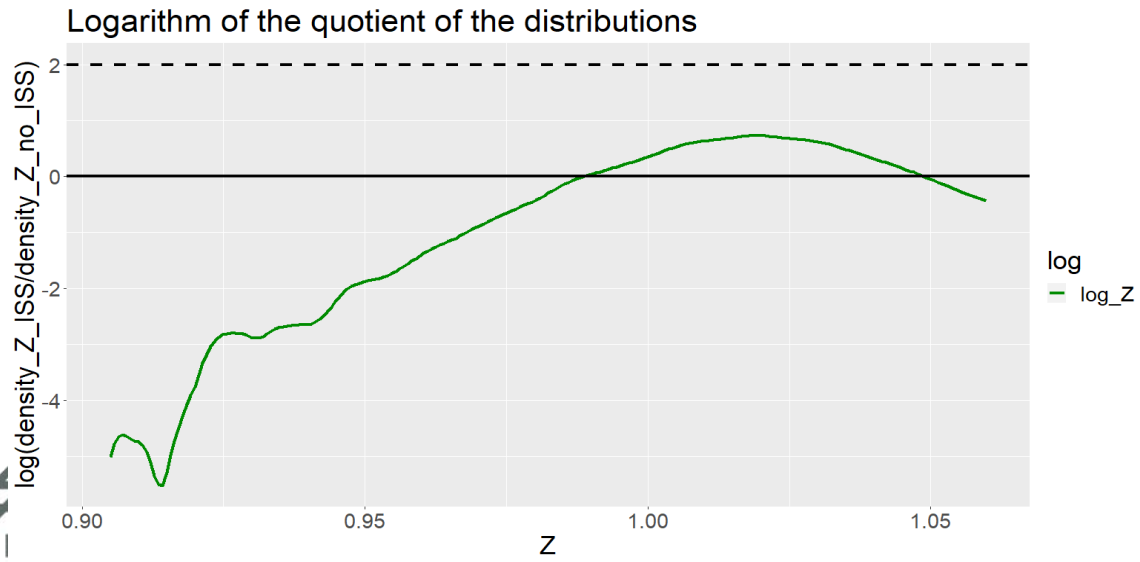

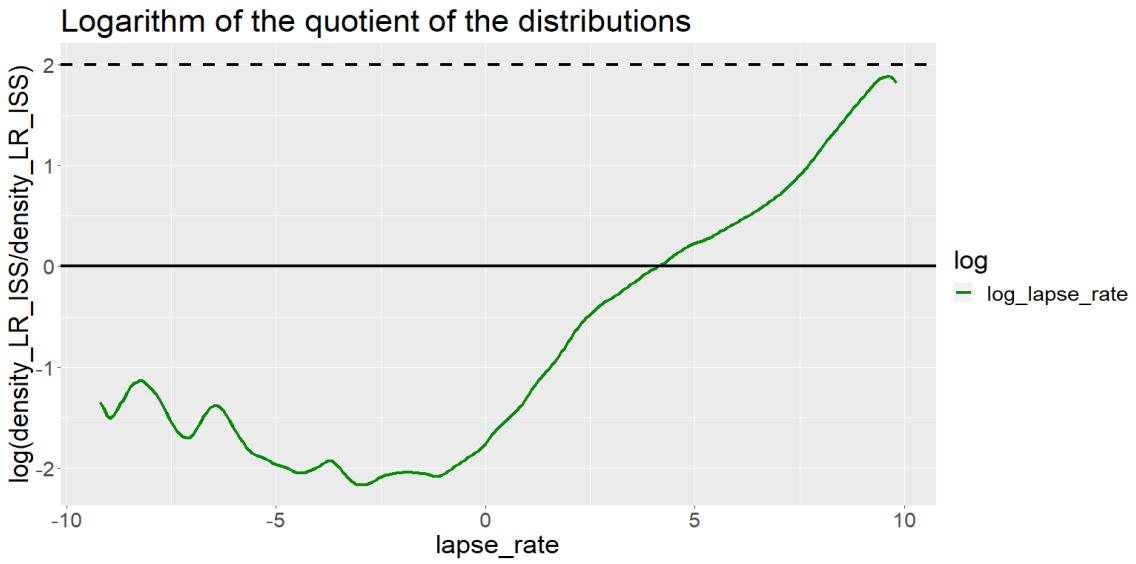

log-likelihood ratios for dynamical quantities: ω, div, T, RHi(era5)

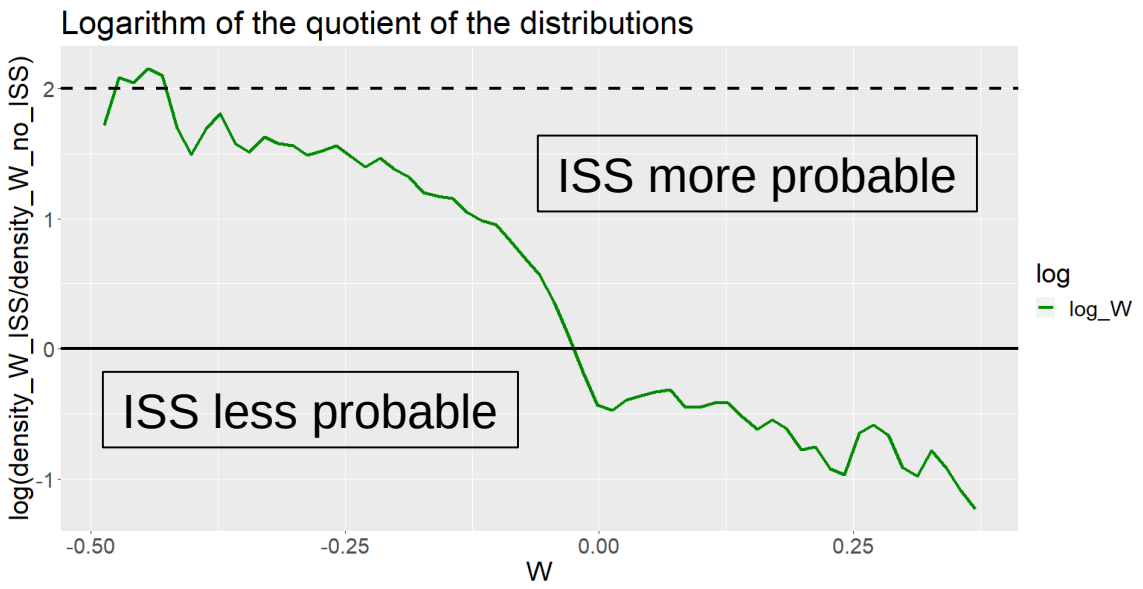

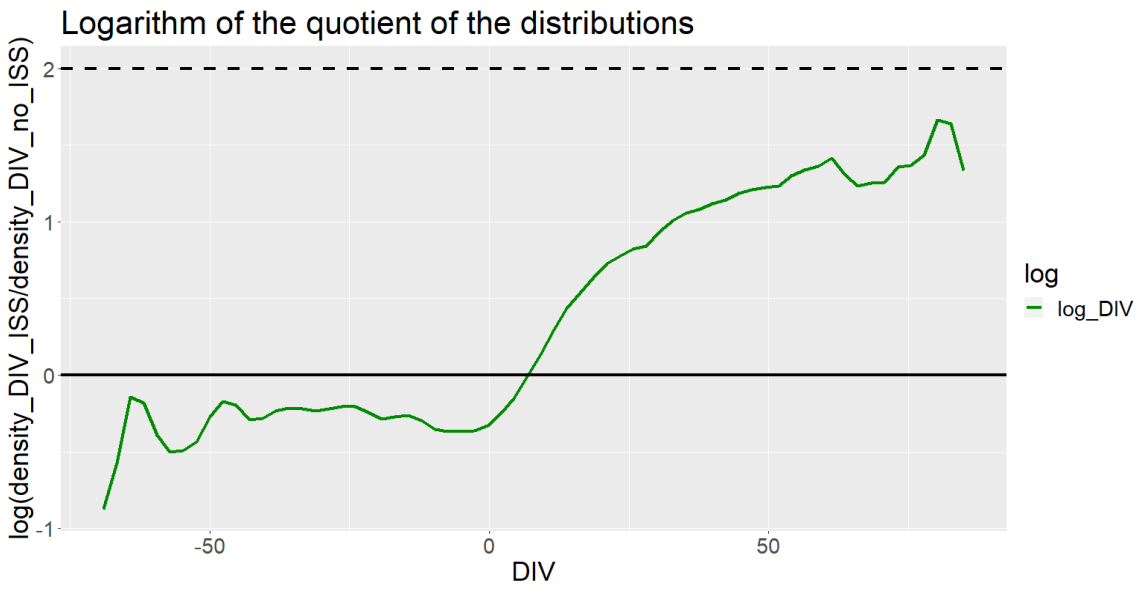

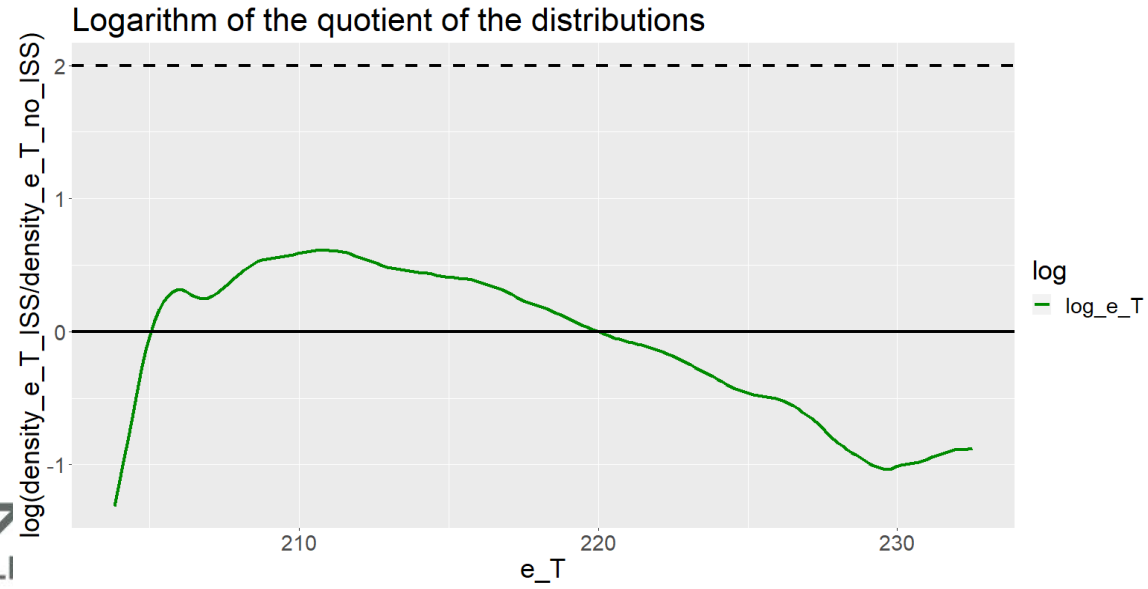

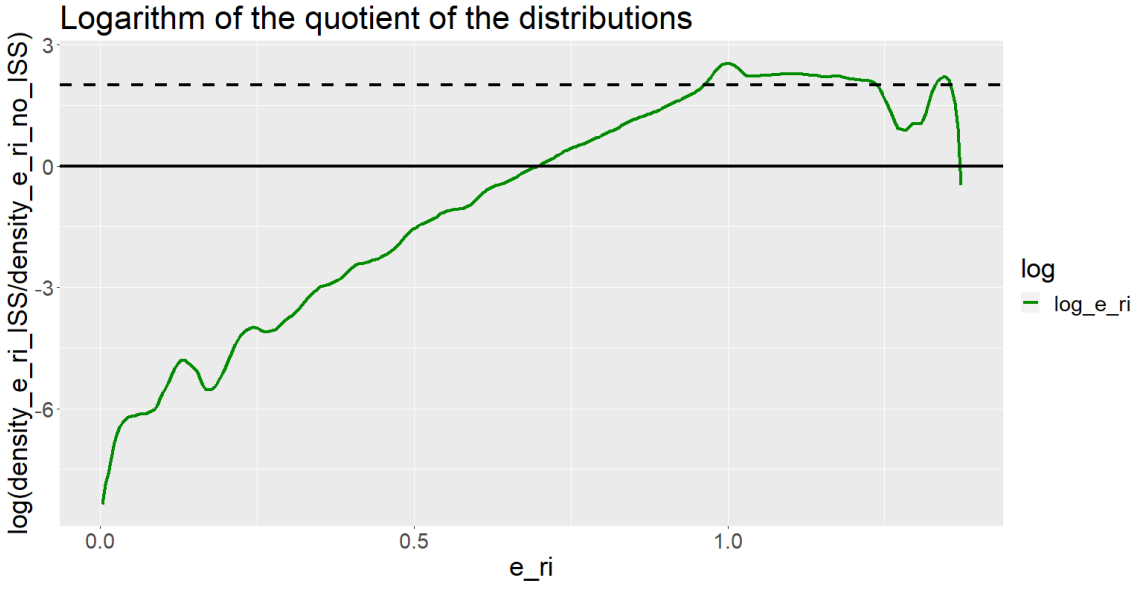

What can we learn about supersaturation from dynamical quantities (2)

How to decide whether a quantity X is generally advantageous to help in the prediction of ISS?

We can take the expectation value of the log-likelihood ratio, which leads to the so-called **Kullback-Leibler divergence**

$$D_{KL}\left(F_{X|ISS} \parallel F_{X|\neg ISS}\right) = \int f_X(x|ISS) \log \frac{f_X(x|ISS)}{f_X(x|\neg ISS)} \mathrm{d}x$$

However, for learning, both significantly positive and negative log-likelihoods are important, thus it is not good that these contributions more or less cancel in the integral. Thus we will use the absolute value of the logit:

$$E_{AL}\left(F_{X|ISS} \parallel F_{X|\neg ISS}\right) = \int f_X(x|ISS) \left|\log \frac{f_X(x|ISS)}{f_X(x|\neg ISS)}\right| \mathrm{d}x$$

Note that E_{AL} (expectation of absolute logit) is an asymmetric quantity, with $f_X(x|ISS)$ as the weighting function. One can also exchange the two conditional densities and additionally one can use the mean value of these two quantities to yield a symmetric quantity.

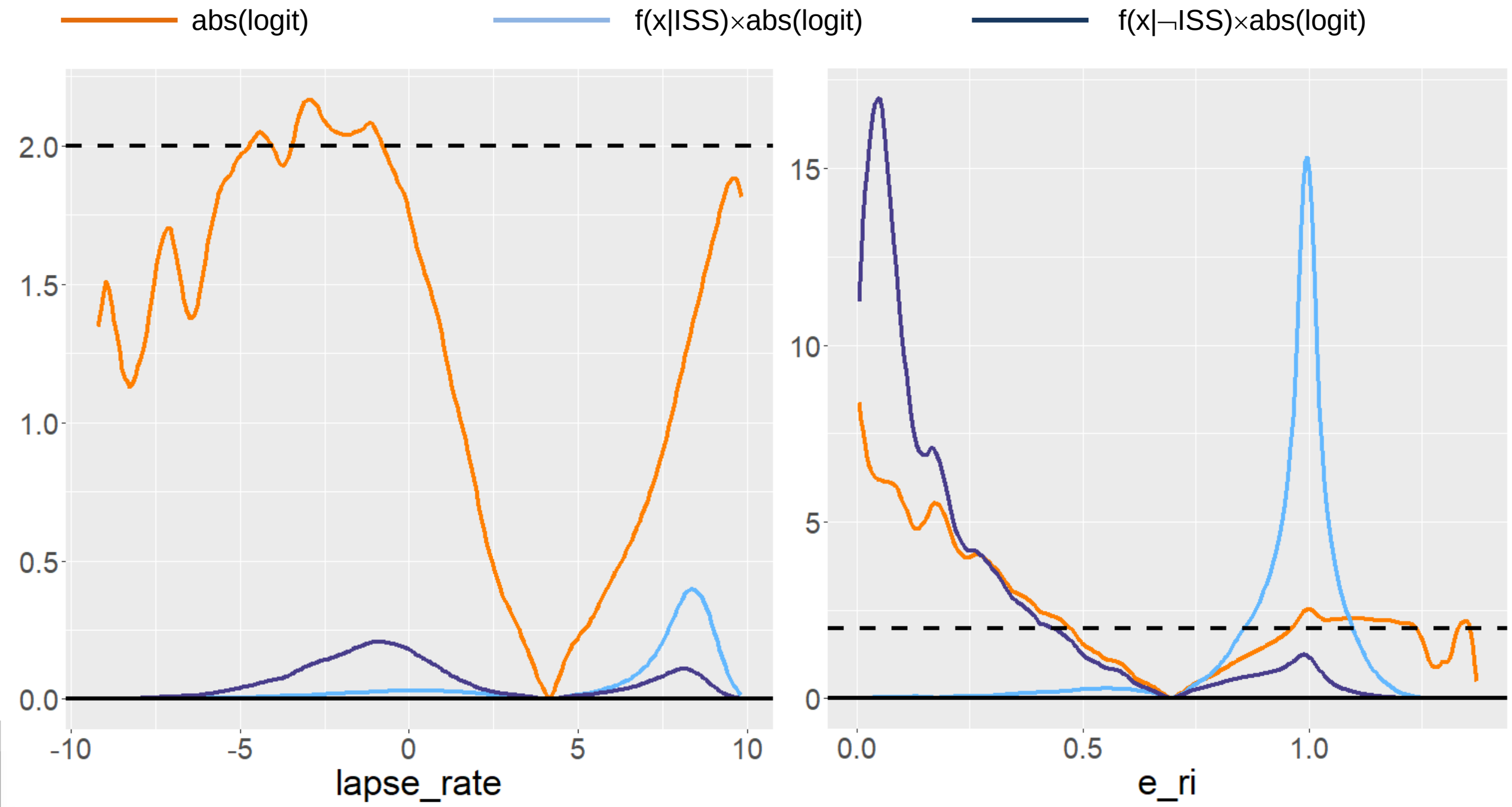
abs(logit)
f(x|ISS)×abs(logit)
f(x|¬ISS)×abs(logit)
2.0
1.5
1.0
0.5
0.0
-10
-5
0
5
10
lapse_rate
15
10
5
0
0.0
0.5
1.0
e_ri

Expectation values of abs(log-likelihood) for various quantities

quantity	ISS	¬ISS
e_ri	1.75	3.41
T	0.34	0.38
ω	0.56	0.43
DIV	0.42	0.33
ζ	0.96	1.20
PV	0.90	2.07
γ	0.96	1.24
Z	0.52	0.88

Application: Probability of ice supersaturation in various (e_ri,γ) situations

P(ISS); x: e_ri, y: LR

LR \ e_ri	0.0-0.1	0.1-0.2	0.2-0.3	0.3-0.4	0.4-0.5	0.5-0.6	0.6-0.7	0.7-0.8	0.8-0.9	0.9-1.0	1.0-1.1	1.1-1.2	1.2-1.3	1.3-1.4
-14.0- -13.0														
-13.0- -12.0														
-12.0- -11.0														
-11.0- -10.0		0.00	0.00	0.00	0.00	0.00	0.00							
-10.0- -9.0	0.00	0.00	0.00	0.00	0.02	0.00	0.00	0.14	0.20					
-9.0- -8.0	0.00	0.00	0.00	0.00	0.00	0.01	0.08	0.21	0.17	0.50				
-8.0- -7.0	0.00	0.00	0.00	0.00	0.00	0.04	0.06	0.05	0.44	0.47	0.33			
-7.0- -6.0	0.00	0.00	0.00	0.00	0.00	0.01	0.08	0.23	0.22	0.51	0.72			
-6.0- -5.0	0.00	0.00	0.00	0.00	0.01	0.02	0.04	0.13	0.29	0.32	0.67			
-5.0- -4.0	0.00	0.00	0.00	0.01	0.01	0.02	0.07	0.15	0.21	0.36	0.40	0.40		
-4.0- -3.0	0.00	0.00	0.00	0.00	0.01	0.02	0.07	0.16	0.27	0.38	0.47	0.69		
-3.0- -2.0	0.00	0.00	0.00	0.00	0.01	0.03	0.07	0.16	0.27	0.42	0.54	0.58		
-2.0- -1.0	0.00	0.00	0.00	0.00	0.01	0.04	0.08	0.16	0.26	0.37	0.50	0.53		
-1.0- 0.0	0.00	0.00	0.00	0.00	0.01	0.04	0.07	0.17	0.30	0.38	0.41	0.48		
0.0-1.0	0.00	0.00	0.00	0.00	0.01	0.03	0.09	0.18	0.30	0.41	0.53	0.51		
1.0-2.0	0.00	0.00	0.00	0.00	0.01	0.04	0.08	0.19	0.32	0.42	0.50	0.48		
2.0-3.0	0.00	0.00	0.00	0.01	0.02	0.06	0.10	0.18	0.29	0.44	0.50	0.40	0.50	
3.0-4.0	0.00	0.00	0.00	0.01	0.02	0.05	0.11	0.20	0.29	0.44	0.52	0.55	0.43	
4.0-5.0	0.00	0.00	0.00	0.01	0.03	0.04	0.12	0.20	0.31	0.48	0.52	0.59	0.44	
5.0-6.0	0.00	0.00	0.00	0.01	0.02	0.05	0.11	0.19	0.29	0.46	0.54	0.56	0.38	
6.0-7.0	0.00	0.00	0.01	0.02	0.02	0.04	0.11	0.19	0.32	0.49	0.58	0.59	0.51	
7.0-8.0	0.00	0.00	0.00	0.01	0.02	0.04	0.08	0.16	0.32	0.52	0.62	0.61	0.63	
8.0-9.0	0.00	0.00	0.01	0.01	0.02	0.03	0.08	0.18	0.31	0.56	0.65	0.64	0.69	
9.0-10.0			0.00	0.04	0.00	0.06	0.08	0.21	0.34	0.58	0.67			

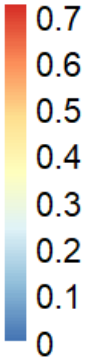

Conclusions

- All kinds of ice clouds require ice supersaturation in their formation;
- Forecasting of ice supersaturation is challenging for a multitude of reasons;

- Upper-tropospheric humidity is a measure of vertically averaged humidity, not of local RHi;
- Contribution and weighting functions of RT theory show where detected photons originate and what the mean properties of the emitting/scattering layers are;

- Ice supersaturation occurs preferentially in ascending air streams connected with the jet stream or with orographically excited waves, but seemingly as well on the top of anticyclonical systems with less pronounced vertical motion.
- Lapse rates within ISSRs are particularly large, temperature profiles below ISSRs particularly steep.

- Distributions of dynamical quantities conditioned on supersaturation or not differ substantially. This may allow a probabilistic prediction of ISS as long as we must wait for better humidity measurements in the UT and better parameterisations of stratiform cirrus in weather forecast models.

Further reading

- Gierens, K., K. Eleftheratos, 2017: Technical note: On the intercalibration of HIRS channel 12 brightness temperatures following the transition from HIRS 2 to HIRS 3/4 for ice saturation studies. Atmos. Meas. Tech., 10, 681–693.
- Gierens, K., K. Eleftheratos, 2019: On the interpretation of upper-tropospheric humidity based on a second-order retrieval from infrared radiances. Atmos. Chem. Phys., 19, 3733-3746.
- Gierens, K. K. Eleftheratos, 2021: The contribution and weighting functions of radiative transfer - theory and application to the retrieval of upper-tropospheric humidity. Meteorol. Z., 30, 79-88.
- Kästner, M. und Meyer, R. und Wendling, P. (1999) Influence of Weather Conditions on the Distribution of Persistent Contrails. Meteorological Applications, 6, Seiten 261-271
- Immler, F.; Treffeisen, R.; Engelbart, D.; Krüger, K.; Schrems, O. Cirrus, contrails, and ice supersaturated regions in high pressure systems at northern mid latitudes. Atmos. Chem. Phys. 2008, 8, 1689–1699.
- Spichtinger, P., K. Gierens, H. Wernli, 2005: A case study on the formation and evolution of ice supersaturation in the vicinity of a warm conveyor belt's outflow region. Atmos. Chem. Phys., 5, 973-987
- Irvine, E. A., B. J. Hoskins, and K. P. Shine (2014), A Lagrangian analysis of ice-supersaturated air over the North Atlantic, J. Geophys. Res. Atmos., 119, 90–100, doi:10.1002/2013JD020251
- Gierens, K., L. Wilhelm, S. Hofer, S. Rohs, 2022: The effect of ice supersaturation and thin cirrus on lapse rates in the upper troposphere. Atmos. Chem. Phys. 22, 7699-7712. doi.org/10.5194/acp-22-7699-2022.
- Gierens, K., S. Brinkop, 2012: Dynamical characteristics of ice supersaturated regions. Atmos. Chem. Phys., 12, 11933-11942.
- Wilhelm, L., K. Gierens, S. Rohs, 2022: Meteorological Conditions that Promote Persistent Contrails. Appl. Sci. 2022, 12, 4450. doi.org/10.3390/app12094450.

END